Semi-Global Sampled-Data Dynamic Output Feedback Controller for the Glucose-Insulin System

M. Di Ferdinando P. Pepe P. Palumbo S. Panunzi A. De Gaetano

***Abstract*—In this paper we deal with the problem of tracking a desired plasma glucose concentration by means of intra-venous insulin administration, for Type 2 diabetic patients exhibiting basal hyperglycemia. A nonlinear time-delay model is used to describe the glucose-insulin regulatory system, according to which a model-based approach is exploited to design a semi-global sampled-data dynamic output feedback controller. It is shown that emulation, by Euler approximation, of a proposed continuous-time control law yields stabilization in the sample-and-hold sense to the closed-loop system. The glucose regulator makes use of only sampled glucose measurements. Theoretical results are validated through a virtual environment broadly accepted as a substitute to animal trials for the preclinical testing of control strategies in plasma glucose regulation. Numerical results are encouraging and pave the way to further clinical verifications.**

***Index Terms*—Nonlinear sampled-data control, Nonlinear time-delay system, Stabilization in the Sample-and-Hold sense, Glucose-Insulin model, *In silico* validation.**

I. Introduction

Diabetes Mellitus (DM) is a chronic disease, whose alarming continuous growth has been estimated by the International Diabetes Federation (IDF) to involve currently 415 million patients worldwide (a number predicted to rise up to 642 million by 2040), with a total health expenditure due to diabetes estimated at 673 billion US dollars [29]. DM is in fact a group of metabolic disorders characterized by sustained hyperglycemia, mainly involving insulin, the primal hormone responsible of plasma glucose homeostasis. In case of a total lack of insulin we deal with Type 1 DM (T1DM) and patients require exogenous insulin administration throughout their lifetime. In case of an inadequate compensatory insulin secretory response, possibly combined to a resistance to insulin action, we deal with Type 2 DM (T2DM). Though less severe than T1DM, T2DM accounts for 85% to 95% of all cases of diabetes, thus having a relevant impact in worldwide National Health Systems, since an untimely control of hyperglycemia facilitates the emergence of many and diverse diabetic complications like retinopathy, neuropathy, nefropathy, etc., in both T1DM and T2DM.

This work is supported in part by Atheneum RIA Project 2017 and by the MIUR Project FFABR 2017.

M. Di Ferdinando and Pierdomenico Pepe are with the Department of Information Engineering, Computer Science, and Mathematics, University of L'Aquila, L'Aquila, Italy (e-mail: pierdomenico.pepe@univaq.it, mario.diferdinando@graduate.univaq.it).

P. Palumbo, S. Panunzi and A. De Gaetano are with the Institute of Systems Analysis and Computer Science, National Research Council, Rome, Italy (e-mail: pasquale.palumbo@iasi.cnr.it, simona.panunzi@biomatematica.it, andrea.degaetano@biomatematica.it).

The Artificial Pancreas (AP) refers to the set of integrated systems combining the design of the insulin infusion therapy, the actuators in charge of its delivery (insulin pumps) and the sensor equipments providing measurements to the controller in order to synthesize the closed-loop control law. Most of the available AP results actually involve T1DM (see, among the others, [7], [14], [18], [21], [23], [44] and references therein).

This work investigates closed-loop glucose control therapies for T2DM patients, by means of a model-based approach, that means the control law is synthesized by properly exploiting the mathematical model of the glucose-insulin system. The chosen model is a Delay Differential Equation (DDE) model, published in [31], [34]: motivation is that DDE models are known to properly account for the endogenous insulin delivery rate [24], [30], which cannot be neglected for T2DM. Moreover, the DDE model here adopted has already been shown to be effective in designing model-based, observer-based or, in general, output dynamic glucose control laws [1], [32], [33] according to continuous glucose measurements and continuous insulin administration.

Differently from [32], [33], here the proposed regulator is synthesized according to a novel control design architecture, on the ground of sampled-data measurements (sampled-data regulator). Preliminary results have been proposed in [39] where a *local* sampled-data control law for the nonlinear DDE model is presented. In [13] a *semi-global* sampled-data controller for the glucose-insulin system is provided. In [39] and [13] both measurements of glucose and insulin concentrations are required by the controller, thus making these works just a proof of concept since, unfortunately, insulin measurements cannot be exploited in real-time closed-loop algorithms because they are time-consuming and cumbersome to achieve. This drawback is, here, overcome since the design of the proposed *semi-global* nonlinear sampled-data control law makes use of only plasma glucose measurements. To the best of our knowledge, this problem has never been addressed in the literature.

Insulin is supposed to be intravenously administered: the intravenous route provides a wider range of possible strategies with respect to the subcutaneous route, and ensures a rapid delivery with negligible delays. As a matter of fact, control algorithms based on intravenous infusions (we can cite, among the others, [4], [15], [19], [32], [33], [41]) are directly applicable so far only to problems of glycemia stabilization in critically ill subjects, such as in surgical Intensive Care Units after major procedures, [42].

Sampled-data stabilization has been studied in the literature according to many approaches, such as: i) the time-varying

delay approach (see for instance [17]), ii) the approximate system discretization approach (see [26], [27]), iii) the hybrid system approach (see [2], [28]); iv) the stabilization in the sample-and-hold sense approach (see [5], [6], [12], [10], [11], [36], [38], [37]). To implement sample-data regulators by emulation is often the common choice in practical applications, and its philosophy is shared by some of the aforementioned approaches, like the hybrid and the sample-and-hold sense ones. In these frameworks, emulation consists in (i) first designing a continuous-time controller for the system at hand, and then, (ii) discretizing it in order to make use of sampled-data measurements and to apply the control law by zero-order hold devices. The notion of stabilization in the sample-and-hold sense, introduced in 1997 in [6], has been widely studied for systems described by ordinary differential equations, and recently extended to systems with delays too (see [12], [10], [36] and [38]). Based on these recent results, the sampled-data (by Euler emulation) output dynamic regulator is applied, in this paper, to the DDE model of the glucose-insulin system with the aim of glucose control. It is proved that the proposed sampled-data controller ensures the practical stability of the closed-loop glucose-insulin system, with arbitrary small steady-state error. The proposed *semi-global* sampled-data controller makes use of only glucose measurements in order to perform the glucose reference tracking.

To evaluate the goodness of the proposed control law a population of virtual patients has been created, according to a comprehensive multi-compartmental model of the glucose-insulin system [9] which allows to model healthy subjects as well as T2DM patients and, along with [8], provides the base for the *in silico* subjects of the UVA/PADOVA Type 1 Diabetes Simulator [20], accepted by the FDA (Food and Drug Administration) as a substitute to animal trials for insulin administration therapies. The use of comprehensive models straightforwardly to design the control law would be prohibitive: from the model parameter identification viewpoint, such models include many internal states, usually not easily accessible to have measurements unless of invasive procedures, thus preventing the applicability to individualized therapies; from the other hand, they are associated to high-dimensional differential equations systems, so making it extremely hard to design an easy-to-handle mathematical control law guaranteeing (at least theoretically) the required performances. The use of two distinct mathematical models (one *compact* to design the control law, the other *comprehensive* to validate the AP therapy) has been recently exploited in [25], where the *compact* model was a simplified (linearized, discretized) version of the same *comprehensive* model here adopted. Such a design/validation AP architecture has been proposed in [33], according to the same choice of the compact and comprehensive models, but exploiting a different problem setting and by means of a different control theory design.

Similarly to the virtual environmental benchmark proposed in [33], we design the parameters of the regulator by closing the loop on the DDE model *tailored* to the average virtual patient of the population built up according to the adopted comprehensive model. Then, a massive campaign of simulations is carried out by keeping the control law parameters fixed for any virtual patient sampled from the rather heterogenous population. The effectiveness of the proposed control scheme is validated in terms of safety robustness and performance efficiency [3], by properly accounting for measurements uncertainties and actuators malfunctioning.

A. Notation

$\mathbb{N}$ denotes the set of nonnegative integer numbers, $\mathbb{R}$ denotes the set of real numbers, $\mathbb{R}^\star$ denotes the extended real line $[-\infty,+\infty]$, $\mathbb{R}^+$ denotes the set of nonnegative reals $[0,+\infty)$. The symbol $|\cdot|$ stands for the Euclidean norm of a real vector, or the induced Euclidean norm of a matrix. For a positive integer n, for a positive real Δ, a Lebesgue measurable function $f:[-\Delta,0]\to\mathbb{R}^n$ is said to be essentially bounded if $ess\sup_{t\in[-\Delta,0]}|f(t)|<+\infty$, where $ess\sup_{t\in[-\Delta,0]}|f(t)|=\inf\{a\in R^*:\lambda(\{t\in[-\Delta,0]:|u(t)|>a\})=0\}$, λ denoting the Lebesgue measure. The essential supremum norm of an essentially bounded function is indicated with the symbol $\|\cdot\|_\infty$. For a positive integer n, for a positive real Δ (maximum involved time-delay): $\mathcal{C}^n$ and $W_n^{1,\infty}$ denote the space of the continuous functions mapping $[-\Delta,0]$ into $\mathbb{R}^n$ and the space of the absolutely continuous functions, with essentially bounded derivative, mapping $[-\Delta,0]$ into $\mathbb{R}^n$, respectively. For a positive real p, for $\phi\in\mathcal{C}^n$, $\mathcal{C}_p^n(\phi)=\{\psi\in\mathcal{C}^n:\|\psi-\phi\|_\infty\le p\}$. The symbol $\mathcal{C}_p^n$ denotes $\mathcal{C}_p^n(0)$. For a continuous function $x:[-\Delta,c)\to\mathbb{R}^n$, with $0<c\le+\infty$, for any real $t\in[0,c)$, x_t is the function in $\mathcal{C}^n$ defined as $x_t(\tau)=x(t+\tau)$, $\tau\in[-\Delta,0]$. For a positive integer n, $C^1(\mathbb{R}^n;\mathbb{R}^+)$ denotes the space of the continuous functions from $\mathbb{R}^n$ to $\mathbb{R}^+$, admitting continuous (partial) derivatives; $C_L^1(\mathbb{R}^n;\mathbb{R}^+)$ denotes the subset of the functions in $C^1(\mathbb{R}^n;\mathbb{R}^+)$ admitting locally Lipschitz (partial) derivatives; $C^1(\mathbb{R}^+;\mathbb{R}^+)$ denotes the space of the continuous functions from $\mathbb{R}^+\to\mathbb{R}^+$, admitting continuous derivative; $C_L^1(\mathbb{R}^+;\mathbb{R}^+)$ denotes the subset of functions in $C^1(\mathbb{R}^+;\mathbb{R}^+)$ admitting locally Lipschitz derivative. Let us here recall that a continuous function $\gamma:\mathbb{R}^+\to\mathbb{R}^+$ is: of class $\mathcal{P}_0$ if $\gamma(0)=0$; of class $\mathcal{P}$ if it is of class $\mathcal{P}_0$ and $\gamma(s)>0$, $s>0$; of class $\mathcal{K}$ if it is of class $\mathcal{P}$ and strictly increasing; of class $\mathcal{K}_\infty$ if it is of class $\mathcal{K}$ and unbounded. The symbol I_d denotes the identity function in $\mathbb{R}^+$. For a given positive integer n, for a symmetric, positive definite matrix $P\in\mathbb{R}^{n\times n}$, $\lambda_{max}(P)$ and $\lambda_{min}(P)$ denote the maximum and the minimum eigenvalue of P, respectively. The symbol $\circ$ denotes composition (of functions). For positive integers n, m, for a map $f:\mathcal{C}^n\times\mathbb{R}^m\to\mathbb{R}^n$, and for a locally Lipschitz functional $V:\mathcal{C}^n\to\mathbb{R}^+$, the derivative in Driver's form (see [35] and the references therein) $D^+V:\mathcal{C}^n\times\mathbb{R}^m\to\mathbb{R}^\star$, of the functional V, is defined, for $\phi\in\mathcal{C}^n$, $u\in\mathbb{R}^m$, as:

$$D^+V(\phi,u)=\limsup_{h\to0^+}\frac{V(\phi_{h,u})-V(\phi)}{h},\qquad(1)$$

where, in the case of $\Delta>0$, for $0\le h<\Delta$, $\phi_{h,u}\in\mathcal{C}^n$ is defined, for $s\in[-\Delta,0]$, as

$$\phi_{h,u}(s)=\begin{cases}\phi(s+h), & s\in[-\Delta,-h),\\ \phi(0)+(s+h)f(\phi,u), & s\in[-h,0].\end{cases}$$

II. The DDE Glucose-insulin model

Define $G(t)$, [mM], and $I(t)$, [pM], plasma glucose and insulin concentrations. The nonlinear DDE model, [31], [34], exploited to design the closed-loop control law is

$$\begin{aligned}
&\dot{G}(t) = -K_{xgi}G(t)I(t) + \frac{T_{gh}}{V_G} + \frac{d(t)}{V_G},\\
&\dot{I}(t) = -K_{xi}I(t) + \frac{T_{iGmax}}{V_I}\varphi(G(t-\tau_g)) + \frac{v(t)}{V_I},\\
&\bar{y}_j = G(t_j), \quad j = 0, 1, \ldots\\
&G(\tau) = G_0(\tau) \quad I(\tau) = I_0(\tau) \quad \tau \in [-\tau_g, 0],
\end{aligned} \tag{2}$$

where K_{xgi}, [$\text{min}^{-1}\text{pM}^{-1}$], is the insulin-dependent glucose uptake rate per pM of plasma insulin concentration, T_{gh}, [min^{-1}(mmol/kgBW)], is the net balance between hepatic glucose output and insulin-independent zero-order glucose tissue uptake, V_G and V_I, [L/kgBW], are the distribution volumes for glucose and insulin, K_{xi}, [min^{-1}], is the constant elimination rate for insulin, T_{iGmax}, [min^{-1}(pmol/kgBW)], is the maximal rate of second-phase insulin release, $\varphi(\cdot)$ models the endogenous pancreatic insulin delivery rate according to the following sigmoidal function:

$$\varphi(G(t-\tau_g)) = \frac{\left(\frac{G(t-\tau_g)}{G^*}\right)^{\gamma}}{1+\left(\frac{G(t-\tau_g)}{G^*}\right)^{\gamma}}; \tag{3}$$

with γ the sigmoidal function parameter related to the steepness of φ, G^*, [mM], the glycemia at which the insulin release is the half of its maximal rate and τ_g, [min], the apparent delay with which the pancreas varies its secondary insulin release in response to varying plasma glucose concentrations. The pair $(G_0(\tau), I_0(\tau))$ is the initial condition of the model, corresponding to the plasma glucose/insulin concentrations before the control input is applied. They can be taken equal to the constant basal levels (G_b, I_b).

$d(t)$, [(mmol/kgBW)/min], is an exogenous disturbance affecting glucose dynamics, usually associated to meals or physical exercise. It will be neglected for the control law synthesis. $v(t)$, [(pmol/kgBW)/min], is the exogenous intravenous insulin delivery rate, i.e., the control input. $\bar{y}_j$ [mM], are the sampled glucose measurement i.e., the output signal at sampling times t_j, $j = 0, 1, 2, ...$

Let G_{ref} be the desired glucose reference, the one to be tracked by the control law. The choice of a desired glucose level G_{ref} leads to the definition of the insulin and input references, I_{ref} and v_{ref}, respectively

$$\begin{aligned}
I_{ref} &= \frac{T_{gh}}{V_G G_{ref} K_{xgi}}\\
v_{ref} &= V_I I_{ref} K_{xi} - T_{iGmax}\varphi(G_{ref}).
\end{aligned} \tag{4}$$

The pair (G_{ref}, I_{ref}) refers to the steady state solution achieved by fixing $v(t) \equiv v_{ref}$, $t \geq 0$.

III. Design of the semi-global sampled-data output controller for the glucose-insulin system

In [13], a preliminary result on a *global* nonlinear sampled-data regulator for the glucose-insulin system is provided, with the drawback of a complete knowledge of the state of the system, i.e. the implementation of the control strategy provided in [13] requires both glucose and insulin measurements. Unfortunately, insulin measurements are less accurate than glucose measurements and time-consuming to obtain, thus inappropriate to be exploited in a real-time closed-loop control algorithm. Then, there is a need to design the output dynamic controller based on only glucose measurements. According to the emulation approach, with a little abuse of notation, we will associate to the sequence $\bar{y}_j$, $j = 0, 1, \ldots$, a continuous fictitious output signal $\bar{y}(t) = G(t)$ (i.e. the output is supposed to be acquired continuously in time). No meals are supposed for the control design, therefore $d(t) \equiv 0$ in (2).

By properly exploiting the theory on the stabilization in the sample-and-hold sense (see [5], [6]), as applied to time-delay systems (see [12], [36] and [38]), a *semi-global* nonlinear sampled-data output controller for system (2) is designed in order to reduce the high basal plasma glucose concentration to the reference glucose value.

In the spirit of emulation, we first propose the following continuous-time output dynamic controller for (2):

$$\begin{aligned}
\dot{\widehat{G}}(t) &= -K_{xgi}\widehat{G}(t)\widehat{I}(t) + \frac{T_{gh}}{V_G} + H_1(\bar{y}(t) - \widehat{G}(t)),\\
\dot{\widehat{I}}(t) &= -K_{xi}\widehat{I}(t) + \frac{T_{iGmax}}{V_I}\varphi(\bar{y}(t-\tau_g))\\
&\quad + \frac{v(t)}{V_I} + H_2(\bar{y}(t) - \widehat{G}(t))\\
&\quad + \frac{K_{xgi}}{\rho}\left((\widehat{G}(t) - G_{ref})^2 - (\bar{y}(t) - G_{ref})^2\right),\\
v(t) &= V_I\Big((K_{xi}\widehat{I}(t) - \frac{T_{iGmax}}{V_I}\varphi(\bar{y}(t-\tau_g))\\
&\quad + \frac{K_{xgi}}{\rho}(\bar{y}(t) - G_{ref})^2 - H_2(\bar{y}(t) - G_{ref})\\
&\quad - H_3(\widehat{I}(t) - I_{ref})\Big),\\
\widehat{G}(\tau) &= \widehat{G}_0(\tau), \quad \widehat{I}(\tau) = \widehat{I}_0(\tau), \quad \tau \in [-\tau_g, 0],
\end{aligned} \tag{5}$$

where $H_1, H_2, H_3, \rho \in \mathbb{R}$ are scalar control tuning parameters.

Before to introduce the Euler emulation, we need to formalize the output sampling instants introduced in (2) according to the following definition of partition of $[0, +\infty)$, that we use in the theory of sampled-data systems (see [6] and [36]).

Definition 1: A partition $\pi = \{t_i,\ i = 0, 1, ...\}$ of $[0, +\infty)$ is a countable, strictly increasing sequence t_i, with $t_0 = 0$, such that $t_i \to +\infty$ as $i \to +\infty$. The diameter of π, denoted $diam(\pi)$, is defined as $\sup_{i\geq 0} t_{i+1} - t_i$. The dwell time of π, denoted $dwell(\pi)$, is defined as $\inf_{i\geq 0} t_{i+1} - t_i$. For any positive real $a \in (0, 1]$, $b > 0$, $\pi_{a,b}$ is any partition π with $ab \leq dwell(\pi) \leq diam(\pi) \leq b$.

Given a partition $\pi_{a,\delta} = \{t_j,\ j = 0, 1, ...\}$, the Euler emulation of the output dynamic controller provided in (5) is

described, for $t_j \in \pi_{a,\delta}$, by the following equations

$$\begin{aligned}
\widehat{G}\,(t_{j+1}) &= \widehat{G}\,(t_j) + (t_{j+1}-t_j)\Big(- K_{xgi}\widehat{G}\,(t_j)\,\widehat{I}\,(t_j) \\
&\quad + \frac{T_{gh}}{V_G} + H_1(\bar{y}(t_j) - \widehat{G}\,(t_j))\Big), \\
\widehat{I}\,(t_{j+1}) &= \widehat{I}\,(t_j) + (t_{j+1}-t_j)\Big(- K_{xi}\widehat{I}\,(t_j) \\
&\quad + \frac{T_{iGmax}}{V_I}\varphi\left(\bar{y}\left(t_j - \tau_g\right)\right) \\
&\quad + \frac{v(t_j)}{V_I} + H_2(\bar{y}(t_j) - \widehat{G}\,(t_j)) \\
&\quad + \frac{K_{xgi}}{\rho}\Big((\widehat{G}(t_j) - G_{ref})^2 - (\bar{y}(t_j) - G_{ref})^2\Big)\Big), \\
v(t_j) &= V_I\Big(K_{xi}\widehat{I}\,(t_j) - \frac{T_{iGmax}}{V_I}\varphi\left(\bar{y}\left(t_j - \tau_g\right)\right) \\
&\quad + \frac{K_{xgi}}{\rho}(\bar{y}(t_j) - G_{ref})^2 - H_2(\bar{y}(t_j) - G_{ref}) \\
&\quad - H_3(\widehat{I}(t_j) - I_{ref})\Big).
\end{aligned} \tag{6}$$

Before to state the main theoretical results related to the closed-loop system constituted by the DDE glucose-insulin model (2) in closed-loop with $v(t) = v(t_j)$, $t_j \le t < t_{j+1}$ (see Euler emulation (6)), we introduce the following standard assumptions (see [12], [10], [11], [36], [38], [37]), which will be useful to tune the control parameters.

Assumption 1: Let q an arbitrary given positive real. The initial condition in (2) is such that $\begin{bmatrix} G_0(\tau) - G_{ref} \\ I_0(\tau) - I_{ref} \end{bmatrix}$, $\tau \in [-\tau_g, 0]$, is in $W_2^{1,\infty}$, and

$$ess \sup_{\theta\in[-\tau_g,0]} \left| \frac{d\begin{bmatrix} G_0(\theta) - G_{ref} \\ I_0(\theta) - I_{ref} \end{bmatrix}}{d\theta} \right| \le \frac{q}{\sqrt{2}}. \tag{7}$$

Analogously, the initial condition in (5) is such that $\begin{bmatrix} \widehat{G}_0(\tau) - G_{ref} \\ \widehat{I}_0(\tau) - I_{ref} \end{bmatrix}$, $\tau \in [-\tau_g, 0]$, is in $W_2^{1,\infty}$, and

$$ess \sup_{\theta\in[-\tau_g,0]} \left| \frac{d\begin{bmatrix} \widehat{G}_0(\theta) - G_{ref} \\ \widehat{I}_0(\theta) - I_{ref} \end{bmatrix}}{d\theta} \right| \le \frac{q}{\sqrt{2}}. \tag{8}$$

Assumption 2: There exist a real H_2, and positive reals H_1, H_3, ρ, p_1, p_2, q_1, q_2, q_3, q_4, ω_1, ω_2, ω_3, ω_4, η, μ such that:

$$\Xi_1 + \eta\mu p_1 < 0, \qquad \Xi_2 + \eta\mu\rho p_1 < 0, \tag{9}$$

$$\Xi_3 + \eta\mu p_2 < 0, \qquad \Xi_4 + \eta\mu\rho p_2 < 0 \tag{10}$$

with

$$\Xi_1 = p_1|K_{xgi}G_{ref} + \rho H_2|\omega_1 - 2p_1K_{xgi}I_{ref} + \frac{p_2H_1}{\omega_4} + q_1, \tag{11}$$

$$\Xi_2 = \frac{p_1|K_{xgi}G_{ref} + \rho H_2|}{\omega_1} - 2\rho p_1 K_{xi} + \frac{\rho p_1|K_{xi} - H_3|}{\omega_2} + q_2, \tag{12}$$

$$\begin{aligned}
\Xi_3 &= p_2|K_{xgi}G_{ref} + \rho H_2|\omega_3 - 2p_2K_{xgi}I_{ref} + p_2H_1\omega_4 \\
&\quad - 2p_2H_1 + q_3,
\end{aligned} \tag{13}$$

$$\Xi_4 = \rho p_1|K_{xi} - H_3|\omega_2 + \frac{p_2|K_{xgi}G_{ref} + \rho H_2|}{\omega_3} - 2\rho p_2 H_3 + q_4. \tag{14}$$

Theorem 1: Let Assumptions 1 and 2 hold. Let a be an arbitrary real in $(0, 1]$. Then, for any positive reals R, r with $0 < r < R$, there exist positive reals δ, T, E such that, for any partition $\pi_{a,\delta} = \{t_j,\ j = 0, 1, ...\}$, for any initial condition such that

$$\left| \begin{matrix} G_0(\tau) - G_{ref} \\ I_0(\tau) - I_{ref} \\ \widehat{G}_0(\tau) - G_{ref} \\ \widehat{I}_0(\tau) - I_{ref} \end{matrix} \right| \le R, \quad \tau \in [-\tau_g, 0],$$

the corresponding solution of the sampled-data closed-loop system, described by the equations (see (2), (6))

$$\begin{aligned}
\dot{G}\,(t) &= -K_{xgi}G\,(t)\,I\,(t) + \frac{T_{gh}}{V_G}, \\
\dot{I}\,(t) &= -K_{xi}\big(I\,(t) - \widehat{I}\,(t_j)\,\big) \\
&\quad + \frac{T_{iGmax}}{V_I}(\varphi\left(G\left(t - \tau_g\right)\right) - \varphi\left(G\left(t_j - \tau_g\right)\right) \\
&\quad + \frac{K_{xgi}}{\rho}(G(t_j) - G_{ref})^2 - H_2(G(t_j) - G_{ref}) \\
&\quad - H_3(\widehat{I}(t_j) - I_{ref}), \\
\widehat{G}\,(t_{j+1}) &= \widehat{G}\,(t_j) + (t_{j+1}-t_j)\cdot \\
&\quad \Big(- K_{xgi}\widehat{G}\,(t_j)\,\widehat{I}\,(t_j) + \frac{T_{gh}}{V_G} + H_1(G(t_j) - \widehat{G}\,(t_j))\Big), \\
\widehat{I}\,(t_{j+1}) &= \widehat{I}\,(t_j) + (t_{j+1}-t_j)\Big(- H_2(\widehat{G}\,(t_j) - G_{ref}) \\
&\quad - H_3(\widehat{I}(t_j) - I_{ref}) + \frac{K_{xgi}}{\rho}(\widehat{G}(t_j) - G_{ref})^2)\Big), \\
&t \in [t_j, t_{j+1}), \quad j = 0, 1, ...,
\end{aligned} \tag{15}$$

exists for all $t \in \mathbb{R}^+$, $t_j \in \pi_{a,\delta}$, and, furthermore, satisfies:

$$\left| \begin{matrix} G(t) - G_{ref} \\ I(t) - I_{ref} \\ \widehat{G}(t_j) - G_{ref} \\ \widehat{I}(t_j) - I_{ref} \end{matrix} \right| \le E, \quad \forall t \in \mathbb{R}^+, \quad \forall t_j \in \pi_{a,\delta},$$

$$\left| \begin{matrix} G(t) - G_{ref} \\ I(t) - I_{ref} \\ \widehat{G}(t_j) - G_{ref} \\ \widehat{I}(t_j) - I_{ref} \end{matrix} \right| \le r, \quad \forall t \ge T, \quad \forall t_j \in \pi_{a,\delta}, \quad t_j \ge T. \tag{16}$$

IV. Proof of Theorem 1

The proof is based on recent results on the stabilization in the sample-and-hold sense (see [12], [11], [36]). As a preliminary step it is useful to rewrite system (2) with respect to the displacement

$$x\,(t) = \begin{bmatrix} x_1\,(t) \\ x_2\,(t) \end{bmatrix} = \begin{bmatrix} G\,(t) - G_{ref} \\ I\,(t) - I_{ref} \end{bmatrix}, \tag{17}$$

with the new control input $u(t)$ and the new output signal $y(t)$

$$\begin{array}{l} u\left(t\right)=v\left(t\right)-v_{ref},\\ y(t)=\begin{bmatrix}y_1(t)\\ y_2(t)\end{bmatrix}=\begin{bmatrix}\bar{y}(t)-G_{ref}\\ \bar{y}(t-\tau_g)-G_{ref}\end{bmatrix}=\\ \begin{bmatrix}G(t)-G_{ref}\\ G(t-\tau_g)-G_{ref}\end{bmatrix}=\begin{bmatrix}x_1(t)\\ x_1(t-\tau_g)\end{bmatrix}. \end{array} \tag{18}$$

By letting $x_t(\tau)=\begin{bmatrix}x_{1,t}(\tau)\\ x_{2,t}(\tau)\end{bmatrix}=\begin{bmatrix}G\left(t+\tau\right)-G_{ref}\\ I\left(t+\tau\right)-I_{ref}\end{bmatrix}$, $\tau\in[-\tau_g,0]$, it is:

$$\begin{array}{l} \dot{x}_1\left(t\right)=-K_{xgi}\left(x_1\left(t\right)+G_{ref}\right)\left(x_2\left(t\right)+I_{ref}\right)+\dfrac{T_{gh}}{V_G},\\ \dot{x}_2\left(t\right)=-K_{xi}\left(x_2\left(t\right)+I_{ref}\right)\\ \quad+\dfrac{T_{iGmax}}{V_I}\varphi\left(\left(x_1\left(t-\tau_g\right)+G_{ref}\right)\right)+\dfrac{v_{ref}+u(t)}{V_I},\\ y(t)=\begin{bmatrix}x_1(t)\\ x_1(t-\tau_g)\end{bmatrix},\\ x\left(\tau\right)=x_0\left(\tau\right)=\begin{bmatrix}G_0\left(\tau\right)-G_{ref}\\ I_0\left(\tau\right)-I_{ref}\end{bmatrix},\quad \tau\in\left[-\tau_g,0\right]. \end{array} \tag{19}$$

Notice that system (19) is in the form

$$\begin{array}{l} \dot{x}\left(t\right)=f\left(x_t,u\left(t\right)\right),\quad t\geq 0\quad a.e.,\\ y\left(t\right)=h\left(x_t\right),\\ x\left(\tau\right)=x_0\left(\tau\right),\quad \tau\in\left[-\tau_g,0\right], \end{array} \tag{20}$$

where: $x\left(t\right)\in\mathbb{R}^2$; x_0, $x_t\in\mathcal{C}^2$; τ_g is the involved time delay; $u\left(t\right)\in\mathbb{R}$ is the input; $y\left(t\right)\in\mathbb{R}^2$ is the output; f is a map from $\mathcal{C}^2\times\mathbb{R}$ to $\mathbb{R}^2$, Lipschitz on bounded sets; h is a map from $\mathcal{C}^2$ to $\mathbb{R}^2$, Lipschitz on bounded sets; according to (4): $f\left(0,0\right)=[0\ 0]^T$ and $h(0)=0$. Furthermore, from Assumption 1, the initial state $x_0\in W_2^{1,\infty}$ and $ess\sup_{\theta\in[-\tau_g,0]}\left|\frac{dx_0(\theta)}{d\theta}\right|\leq\frac{q}{\sqrt{2}}$.

Taking into account the new control input and the new output signal in (18), we rewrite the output dynamic controller (5) with respect to the displacements $\widehat{G}(t)-G_{ref}$ and $\widehat{I}(t)-I_{ref}$:

$$\hat{x}\left(t\right)=\begin{bmatrix}\hat{x}_1\left(t\right)\\ \hat{x}_2\left(t\right)\end{bmatrix}=\begin{bmatrix}\widehat{G}\left(t\right)-G_{ref}\\ \widehat{I}\left(t\right)-I_{ref}\end{bmatrix}. \tag{21}$$

By letting $\hat{x}_t(\tau)=\begin{bmatrix}\hat{x}_{1,t}(\tau)\\ \hat{x}_{2,t}(\tau)\end{bmatrix}=\begin{bmatrix}\widehat{G}\left(t+\tau\right)-G_{ref}\\ \widehat{I}\left(t+\tau\right)-I_{ref}\end{bmatrix}$, $\tau\in[-\tau_g,0]$, it is:

$$\begin{array}{l} \dot{\hat{x}}_1\left(t\right)=-K_{xgi}\left(\hat{x}_1\left(t\right)+G_{ref}\right)\left(\hat{x}_2\left(t\right)+I_{ref}\right)+\dfrac{T_{gh}}{V_G}\\ \quad+H_1(y_1(t)-\hat{x}_1(t)),\\ \dot{\hat{x}}_2\left(t\right)=-K_{xi}\left(\hat{x}_2\left(t\right)+I_{ref}\right)\\ \quad+\dfrac{T_{iGmax}}{V_I}\varphi\left(\left(y_2\left(t\right)+G_{ref}\right)\right)+\dfrac{v_{ref}}{V_I}+\dfrac{u(t)}{V_I}\\ \quad+H_2(y_1(t)-\hat{x}_1(t))+\dfrac{K_{xgi}}{\rho}(\hat{x}_1^2(t)-y_1^2(t)),\\ u(t)=V_I\Big(K_{xi}\left(\hat{x}_2\left(t\right)+I_{ref}\right)\\ \quad-\dfrac{T_{iGmax}}{V_I}\varphi\left(\left(y_2\left(t\right)+G_{ref}\right)\right)-\dfrac{v_{ref}}{V_I}\\ \quad+\dfrac{K_{xgi}}{\rho}y_1^2(t)-H_2y_1(t)-H_3\hat{x}_2(t)\Big),\\ \hat{x}\left(\tau\right)=\hat{x}_0\left(\tau\right)=\begin{bmatrix}\widehat{G}_0\left(\tau\right)-G_{ref}\\ \widehat{I}_0\left(\tau\right)-I_{ref}\end{bmatrix},\quad \tau\in\left[-\tau_g,0\right], \end{array} \tag{22}$$

with the control parameters H_1, H_2, H_3 and ρ satisfying the inequalities in Assumption 2. Notice that (22) is in the form

$$\begin{array}{l} \dot{\hat{x}}\left(t\right)=\widehat{f}\left(\hat{x}_t,u\left(t\right),y\left(t\right)\right),\quad t\geq 0,\\ u\left(t\right)=k\left(\hat{x}_t,y(t)\right),\\ \hat{x}\left(\tau\right)=\hat{x}_0\left(\tau\right),\quad \tau\in\left[-\tau_g,0\right], \end{array} \tag{23}$$

where: $\hat{x}\left(t\right)\in\mathbb{R}^2$; $\hat{x}_0$, $\hat{x}_t\in\mathcal{C}^2$; τ_g is the involved time delay; $u\left(t\right)\in\mathbb{R}$ and $y\left(t\right)\in\mathbb{R}^2$ are the input and the output in (20), respectively; the maps $\widehat{f}:\mathcal{C}^2\times\mathbb{R}\times\mathbb{R}^2\to\mathbb{R}^2$ and $k:\mathcal{C}^2\times\mathbb{R}^2\to\mathbb{R}$ are Lipschitz on bounded sets; according to (4) $\widehat{f}\left(0,0,0\right)=[0\ 0]^T$ and $k\left(0,0\right)=0$. Furthermore, from Assumption 1, the initial state $\hat{x}_0\in W_2^{1,\infty}$, and that $ess\sup_{\theta\in[-\tau_g,0]}\left|\frac{d\hat{x}_0(\theta)}{d\theta}\right|\leq\frac{q}{\sqrt{2}}$ (see [12] for more details).

The continuous-time closed-loop system (19), (22) is, thus, described by the following DDE system:

$$\begin{array}{l} \dot{x}_1\left(t\right)=-K_{xgi}\left(x_1\left(t\right)+G_{ref}\right)\left(x_2\left(t\right)+I_{ref}\right)+\dfrac{T_{gh}}{V_G},\\ \dot{x}_2\left(t\right)=-K_{xi}\left(x_2\left(t\right)-\hat{x}_2\left(t\right)\right)+\dfrac{K_{xgi}}{\rho}x_1^2\left(t\right)-H_2x_1\left(t\right)\\ \quad-H_3\hat{x}_2\left(t\right),\\ \dot{\hat{x}}_1\left(t\right)=-K_{xgi}\left(\hat{x}_1\left(t\right)+G_{ref}\right)\left(\hat{x}_2\left(t\right)+I_{ref}\right)+\dfrac{T_{gh}}{V_G}\\ \quad+H_1(x_1(t)-\hat{x}_1(t)),\\ \dot{\hat{x}}_2\left(t\right)=-H_2\hat{x}_1\left(t\right)-H_3\hat{x}_2\left(t\right)+\dfrac{K_{xgi}}{\rho}\hat{x}_1^2(t), \end{array} \tag{24}$$

that is, by exploiting the compact formalism of (20), (23)

$$\begin{array}{l} \dot{x}\left(t\right)=f\left(x_t,k\left(\hat{x}_t,h\left(x_t\right)\right)\right),\quad t\geq 0,\\ \dot{\hat{x}}\left(t\right)=\widehat{f}\left(\hat{x}_t,k\left(\hat{x}_t,h\left(x_t\right)\right),h\left(x_t\right)\right),\\ x\left(\tau\right)=x_0\left(\tau\right),\quad \hat{x}\left(\tau\right)=\hat{x}_0\left(\tau\right),\quad \tau\in\left[-\tau_g,0\right]. \end{array} \tag{25}$$

According to (22) given a partition $\pi_{a,\delta}=\{t_j,\ j=0,1,...\}$, the Euler emulation of the the output dynamic controller provided in (22) is described, for $t_j\in\pi_{a,\delta}$, by the following equations

$$\begin{array}{l} \hat{x}_1\left(t_{j+1}\right)=\hat{x}_1\left(t_j\right)+\left(t_{j+1}-t_j\right)\Big(-K_{xgi}\left(\hat{x}_1\left(t_j\right)+G_{ref}\right)\\ \quad\cdot\left(\hat{x}_2\left(t_j\right)+I_{ref}\right)+\dfrac{T_{gh}}{V_G}+H_1(y_1(t_j)-\hat{x}_1(t_j))\Big),\\ \hat{x}_2\left(t_{j+1}\right)=\hat{x}_2\left(t_j\right)+\left(t_{j+1}-t_j\right)\Big(-K_{xi}\left(\hat{x}_2\left(t_j\right)+I_{ref}\right)\\ \quad+\dfrac{T_{iGmax}}{V_I}\varphi\left(\left(y_2\left(t_j\right)+G_{ref}\right)\right)+\dfrac{v_{ref}}{V_I}+\dfrac{u(t_j)}{V_I}\\ \quad+H_2(y_1(t_j)-\hat{x}_1(t_j))+\dfrac{K_{xgi}}{\rho}(\hat{x}_1^2(t_j)-y_1^2(t_j))\Big),\\ u(t_j)=V_I\Big(K_{xi}\left(\hat{x}_2\left(t_j\right)+I_{ref}\right)\\ \quad-\dfrac{T_{iGmax}}{V_I}\varphi\left(\left(y_2\left(t_j\right)+G_{ref}\right)\right)\\ \quad-\dfrac{v_{ref}}{V_I}+\dfrac{K_{xgi}}{\rho}y_1^2(t_j)-H_2y_1(t_j)-H_3\hat{x}_2(t_j)\Big). \end{array} \tag{26}$$

Let, as long as the solution of (24) exists,

$$\tilde{x}\left(t\right)=\begin{bmatrix}x_1\left(t\right)\\ x_2\left(t\right)\\ \hat{x}_1\left(t\right)\\ \hat{x}_2\left(t\right)\end{bmatrix}\in\mathbb{R}^4,\quad \tilde{x}_t=\begin{bmatrix}x_{1,t}\\ x_{2,t}\\ \hat{x}_{1,t}\\ \hat{x}_{2,t}\end{bmatrix}\in\mathcal{C}^4. \tag{27}$$

According to (27), the closed-loop system (24) has the form:

$$\begin{aligned}&\dot{\tilde{x}}\left(t\right)=\widetilde{F}\left(\tilde{x}_t\right),\\&\tilde{x}\left(\tau\right)=\tilde{x}_0\left(\tau\right)=\begin{bmatrix}x_0\left(\tau\right)\\\hat{x}_0(\tau)\end{bmatrix},\quad\tau\in\left[-\tau_g,0\right],\end{aligned}\tag{28}$$

with $\widetilde{F}:\mathcal{C}^4\rightarrow\mathbb{R}^4$ Lipschitz on bounded sets and such that $\widetilde{F}\left(0\right)=[0\ 0\ 0\ 0]^T$.

The next and main part of the proof is devoted to show that Theorem 4 in [12] can be applied to the closed-loop system (2), (5), stating that for any positive reals r, R, $0<r<R$, $a\in(0,1]$, there exist positive reals δ, T and E such that, for any partition $\pi_{a,\delta}=\{t_i,\ i=0,1,...\}$, for any initial condition

$$|\tilde{x}_0(\tau)|\leq R,\quad\tau\in[-\tau_g,0],$$

the corresponding solution of the sampled-data closed-loop system, described by the equations (see (19), (26))

$$\begin{aligned}\dot{x}_1\left(t\right)&=-K_{xgi}\left(x_1\left(t\right)+G_{ref}\right)\left(x_2\left(t\right)+I_{ref}\right)+\frac{T_{gh}}{V_G},\\\dot{x}_2\left(t\right)&=-K_{xi}\left(x_2\left(t\right)-\hat{x}_2(t_j)\right)\\&\quad+\frac{T_{iGmax}}{V_I}(\varphi\left(x_1\left(t-\tau_g\right)+G_{ref}\right)\\&\quad-\varphi\left(x_1\left(t_j-\tau_g\right)+G_{ref}\right))+\frac{K_{xgi}}{\rho}x_1^2(t_j)\\&\quad-H_2x_1(t_j)-H_3\hat{x}_2(t_j),\end{aligned}$$

$$\begin{aligned}\hat{x}_1\left(t_{j+1}\right)&=\hat{x}_1(t_j)+(t_{j+1}-t_j)\Big(-K_{xgi}\left(\hat{x}_1\left(t_j\right)+G_{ref}\right)\\&\quad\cdot\left(\hat{x}_2\left(t_j\right)+I_{ref}\right)+\frac{T_{gh}}{V_G}+H_1(x_1(t_j)-\hat{x}_1(t_j))\Big),\\\hat{x}_2\left(t_{j+1}\right)&=\hat{x}_2(t_j)+(t_{j+1}-t_j)(-H_3\hat{x}_2(t_j)-H_2\hat{x}_1(t_j)\\&\quad+\frac{K_{xgi}}{\rho}\hat{x}_1^2(t_j)),\\t&\in\left[t_j,t_{j+1}\right),\quad j=0,1,...,\end{aligned}\tag{29}$$

exists for all $t\in\mathbb{R}^+$, $t_j\in\pi_{a,\delta}$, and, furthermore, satisfies:

$$\left|\begin{matrix}x_1\left(t\right)\\x_2\left(t\right)\\\hat{x}_1\left(t_j\right)\\\hat{x}_2\left(t_j\right)\end{matrix}\right|=\left|\begin{matrix}G(t)-G_{ref}\\I(t)-I_{ref}\\\widehat{G}(t_j)-G_{ref}\\\widehat{I}(t_j)-I_{ref}\end{matrix}\right|\leq E,\quad\forall t\in\mathbb{R}^+,\quad\forall t_j\in\pi_{a,\delta},$$

$$\left|\begin{matrix}x_1\left(t\right)\\x_2\left(t\right)\\\hat{x}_1\left(t_j\right)\\\hat{x}_2\left(t_j\right)\end{matrix}\right|=\left|\begin{matrix}G(t)-G_{ref}\\I(t)-I_{ref}\\\widehat{G}(t_j)-G_{ref}\\\widehat{I}(t_j)-I_{ref}\end{matrix}\right|\leq r,\ \forall t\geq T,\ \forall t_j\in\pi_{a,\delta},\ t_j\geq T.\tag{30}$$

To this end, we recall a class of Lyapunov-Krasovskii functionals, which are very helpful for sampled-data stabilization. In particular, we report the definition concerning *smoothly separable functionals* suitably adapted here to cope with the extended state dimension.

Definition 2: (see [36], [38]) A functional $V:\mathcal{C}^{2n}\rightarrow\mathbb{R}^+$ is said to be smoothly separable if there exist a function $V_1\in C_L^1\left(\mathbb{R}^{2n};\mathbb{R}^+\right)$, a locally Lipschitz functional $V_2:\mathcal{C}^{2n}\rightarrow\mathbb{R}^+$ and functions β_i of class $\mathcal{K}_\infty$, $i=1,2$, such that, for any $\tilde{\phi}\in\mathcal{C}^{2n}$, the following equality/inequalities hold

$$\begin{aligned}&V(\tilde{\phi})=V_1(\tilde{\phi}\left(0\right))+V_2(\tilde{\phi}),\\&\beta_1(|\tilde{\phi}(0)|)\leq V_1(\tilde{\phi}(0))\leq\beta_2(|\tilde{\phi}(0)|).\end{aligned}\tag{31}$$

In order to apply Theorem 4 in [12], we have to check that the following hypothesis is satisfied for (28) (see Assumption 3 in [12]).

Hypothesis. There exist a smoothly separable functional $V:\mathcal{C}^4\rightarrow\mathbb{R}^+$ (complying the notation in Definition 2), functions γ_1, γ_2 of class $\mathcal{K}_\infty$, positive reals η, μ, a function p in $C_L^1\left(R^+;R^+\right)$, of class $\mathcal{K}_\infty$, $\nu\in\{0,1\}$, a function α_3 of class $\mathcal{K}$, such that the following inequalities (with respect to the system described by (28)) hold, for any $\tilde{\phi}\in\mathcal{C}^4$,

$$\gamma_1(|\tilde{\phi}(0)|)\leq V(\tilde{\phi})\leq\gamma_2(\|\tilde{\phi}\|_\infty),\tag{32}$$

$$D^+V(\tilde{\phi},0)\leq-\alpha_3(|\tilde{\phi}(0)|),\tag{33}$$

$$\nu D^+V(\tilde{\phi},0)+\eta D^+p\circ V_1(\tilde{\phi},0)+\eta\mu p\circ V_1(\tilde{\phi}\left(0\right))\leq0.\tag{34}$$

To this aim, let $\tilde{\phi}=[\phi_1\ \phi_2\ \phi_3\ \phi_4]^T$. Taking into account Assumption 2, let $P,Q\in\mathbb{R}^{4\times4}$ be two symmetric positive definite matrices, defined as follows:

$$P=\begin{bmatrix}p_1&0&0&0\\0&\rho p_1&0&0\\0&0&p_2&0\\0&0&0&\rho p_2\end{bmatrix},\quad Q=\begin{bmatrix}q_1&0&0&0\\0&q_2&0&0\\0&0&q_3&0\\0&0&0&q_4\end{bmatrix},\tag{35}$$

Define the function $V_1:\mathbb{R}^4\rightarrow\mathbb{R}^+$ as

$$V_1\left(\tilde{x}\right)=\tilde{x}^TP\tilde{x},\qquad\tilde{x}\in\mathbb{R}^4,\tag{36}$$

the functional $V_2:\mathcal{C}^4\rightarrow\mathbb{R}^+$ as

$$V_2(\tilde{\phi})=\int_{-\tau_g}^{0}\tilde{\phi}\left(\tau\right)^TQ\tilde{\phi}\left(\tau\right)d\tau,\qquad\tilde{\phi}\in\mathcal{C}^4,\tag{37}$$

and the functional $V:\mathcal{C}^4\rightarrow\mathbb{R}^+$ as

$$V(\tilde{\phi})=V_1(\tilde{\phi}\left(0\right))+V_2(\tilde{\phi}),\qquad\tilde{\phi}\in\mathcal{C}^4,\tag{38}$$

with V_1 and V_2 in (36) and (37), respectively. Let β_i, γ_i, $i=1,2$, be the functions of class $\mathcal{K}_\infty$ defined, for $s\in\mathbb{R}^+$, as

$$\beta_1\left(s\right)=\lambda_{min}(P)s^2,\quad\beta_2\left(s\right)=\lambda_{max}(P)s^2.\tag{39}$$

$$\gamma_1\left(s\right)=\lambda_{min}(P)s^2,\ \gamma_2\left(s\right)=\left(\lambda_{max}(P)+\tau_g\lambda_{max}(Q)\right)s^2.\tag{40}$$

The functional V is smoothly separable with the functions β_i, $i=1,2$, in (39) (see Definition 2). Furthermore, the functional V satisfies (32) with the functions γ_i, $i=1,2$ in (40).

Taking into account (28), (38), and according to the model constraints (4), for any $\tilde{\phi} \in \mathcal{C}^4$, the following equalities hold

$$\begin{aligned}
&D^+V(\tilde{\phi},0) = D^+V_1(\tilde{\phi},0) + D^+V_2(\tilde{\phi},0)\\
&= \begin{bmatrix} 2p_1\phi_1(0) & 2\rho p_1\phi_2(0) & 2p_2\phi_3(0) & 2\rho p_2\phi_4(0)\end{bmatrix} \widetilde{F}(\tilde{\phi})\\
&+q_1\phi_1^2(0) + q_2\phi_2^2(0) + q_3\phi_3^2(0) + q_4\phi_4^2(0) - q_1\phi_1^2(-\tau_g)\\
&-q_2\phi_2^2(-\tau_g) - q_3\phi_3^2(-\tau_g) - q_4\phi_4^2(-\tau_g)\\
&= -2p_1K_{xgi}\phi_1^2(0)\phi_2(0) - 2p_1K_{xgi}G_{ref}\phi_1(0)\phi_2(0)\\
&-2p_1K_{xgi}I_{ref}\phi_1^2(0) - 2\rho p_1K_{xi}\phi_2^2(0)\\
&+2\rho p_1K_{xi}\phi_2(0)\phi_4(0) + 2p_1K_{xgi}\phi_1^2(0)\phi_2(0)\\
&-2\rho p_1H_2\phi_1(0)\phi_2(0) - 2\rho p_1H_3\phi_2(0)\phi_4(0)\\
&-2p_2K_{xgi}\phi_3^2(0)\phi_4(0) - 2p_2K_{xgi}G_{ref}\phi_3(0)\phi_4(0)\\
&-2p_2K_{xgi}I_{ref}\phi_3^2(0) + 2p_2H_1\phi_1(0)\phi_3(0)\\
&-2p_2H_1\phi_3^2(0) + 2p_2K_{xgi}\phi_3^2(0)\phi_4(0)\\
&-2\rho p_2H_3\phi_4^2(0) - 2\rho p_2H_2\phi_3(0)\phi_4(0)\\
&+q_1\phi_1^2(0) + q_2\phi_2^2(0) + q_3\phi_3^2(0) + q_4\phi_4^2(0) - q_1\phi_1^2(-\tau_g)\\
&-q_2\phi_2^2(-\tau_g) - q_3\phi_3^2(-\tau_g) - q_4\phi_4^2(-\tau_g).
\end{aligned} \tag{41}$$

Besides a couple of ready simplifications, $D^+V(\tilde{\phi},0)$ can be upper bounded as

$$\begin{aligned}
D^+V(\tilde{\phi},0) \leq\ &\Xi_1\phi_1^2(0) + \Xi_2\phi_2^2(0) + \Xi_3\phi_3^2(0) + \Xi_4\phi_4^2(0)\\
&-q_1\phi_1^2(-\tau_g) - q_2\phi_2^2(-\tau_g) - q_3\phi_3^2(-\tau_g) - q_4\phi_4^2(-\tau_g),
\end{aligned} \tag{42}$$

where Ξ_i, $i = 1,2,3,4$ are defined in Assumption 2. Notice that, the positive reals ω_i, $i = 1,2,3,4$ in Assumption 2 have been exploited in (41) according to the following inequalities

$$\begin{aligned}
2\xi_i\phi_j(0)\phi_k(0) &= 2\xi_i\left(\sqrt{\omega_i}\phi_j(0)\right)\left(\frac{\phi_k(0)}{\sqrt{\omega_i}}\right)\\
&\leq |\xi_i|\left(\omega_i\phi_j^2(0) + \frac{\phi_k^2(0)}{\omega_i}\right),
\end{aligned} \tag{43}$$

with $\xi_1 = -p_1(K_{xgi}G_{ref} + \rho H_2)$, $\xi_2 = \rho p_1(K_{xi} - H_3)$, $\xi_3 = -p_2(K_{xgi}G_{ref} + \rho H_2)$, $\xi_4 = p_2H_1$ and the pair of indexes (j,k) in (43):

$$(j,k) = \begin{cases} (1,2) & \text{for } i = 1\\ (4,2) & \text{for } i = 2\\ (3,4) & \text{for } i = 3\\ (3,1) & \text{for } i = 4 \end{cases} \tag{44}$$

Because of the inequalities in Assumption 2, from (43) it follows that

$$D^+V(\tilde{\phi},0) \leq 0. \tag{45}$$

Let α_3 defined, for $s \in \mathbb{R}^+$, as follows

$$\alpha_3(s) = -\max\{\Xi_1,\Xi_2,\Xi_3,\Xi_4\}s^2, \tag{46}$$

where Ξ_i, $i = 1,2,3,4$ are defined in Assumption 2. From (45), for any $\tilde{\phi} \in \mathcal{C}^4$, also inequality (33) holds with function α_3 in (46). Furthermore, taking into account Assumption 2, from (45) (see also (41) and (42)), we have that, for any $\tilde{\phi} \in \mathcal{C}^4$, $D^+V_1(\tilde{\phi},0) \leq 0$. Let us choose $p = I_d$, and $\nu = 1$. Taking into account (45), for any $\tilde{\phi} \in \mathcal{C}^4$, the following equality/inequalities hold

$$\begin{aligned}
&\nu D^+V(\tilde{\phi},0) + \eta D^+p \circ V_1(\tilde{\phi},0) + \eta\mu p \circ V_1(\tilde{\phi}(0))\\
&= D^+V(\tilde{\phi},0) + \eta D^+V_1(\tilde{\phi},0) + \eta\mu V_1(\tilde{\phi}(0))\\
&\leq D^+V(\tilde{\phi},0) + \eta\mu V_1(\tilde{\phi}(0))\\
&\leq \Xi_1\phi_1^2(0) + \Xi_2\phi_2^2(0) + \Xi_3\phi_3^2(0) + \Xi_4\phi_4^2(0)\\
&\quad -q_1\phi_1^2(-\tau_g) - q_2\phi_2^2(-\tau_g) - q_3\phi_3^2(-\tau_g) - q_4\phi_4^2(-\tau_g)\\
&\quad +\eta\mu(p_1\phi_1^2(0) + \rho p_1\phi_2^2(0) + p_2\phi_3^2(0) + \rho p_2\phi_4^2(0))\\
&= \left(\Xi_1 + \eta\mu p_1\right)\phi_1^2(0) + \left(\Xi_2 + \eta\mu\rho p_1\right)\phi_2^2(0)\\
&\quad + \left(\Xi_3 + \eta\mu p_2\right)\phi_3^2(0) + \left(\Xi_4 + \eta\mu\rho p_2\right)\phi_4^2(0)\\
&\quad -q_1\phi_1^2(-\tau_g) - q_2\phi_2^2(-\tau_g) - q_3\phi_3^2(-\tau_g)\\
&\quad -q_4\phi_4^2(-\tau_g) \leq 0,
\end{aligned} \tag{47}$$

with the last inequality ensured by Assumption 2. From (47) inequality (34) holds, and the hypotheses of Theorem 4 in [12] are satisfied. This fact concludes the proof.

V. Evaluation of the glucose control law on a population of virtual patients

In order to validate the safety and efficacy of the proposed glucose control law, we consider a virtual environment, recently exploited in [33] for the same verification issue, though applied to a completely different closed-loop control strategy. A pivotal role in the proposed benchmark is played by the comprehensive mathematical model used to build up the population of virtual subjects upon which the control law is applied: such model [9] allows to deal with healthy subjects as well as T2DM patients and, along with [8] provides the base for the *in silico* subjects of the UVA/PADOVA Type 1 Diabetes Simulator [20], accepted by the Food and Drug Administration (FDA) as a substitute to animal trials to test insulin administration therapies for the artificial pancreas. Similarly to [33] the virtual environment is achieved according to the following steps.

1) The comprehensive model provides a set of parameters allowing to build a T2DM average Virtual Patient (VP) with $G_b = 8.85$mM and $I_b = 59.85$pM (see Table I in [9].
2) The DDE model parameters are estimated in order to best fit the compact model onto the comprehensive one. Such a step has already been done in [33] according to a virtual clinical experiment (the Intra-Venous Glucose Tolerance Test, IVGTT) usually done to identify minimal models parameters. These parameters have been reported in Table I for the ease of the reader. Notice that the basal glycemia/insulinemia are slightly different than the ones of the average VP because measurements errors were accounted for in the compact model identification procedure;
3) The control law parameters are set for the DDE compact model identified at Step 2), properly accounting for the constraints required by Assumption 2.
4) A population of VPs is sampled by randomly varying the comprehensive model parameters. The greater is their coefficient of variation, the more heterogeneous is supposed the population to be.

5) The proposed control law, tuned according to step 3), is applied to the population of VPs, and performances are assessed.

Remark 1: The first three Steps of the aforementioned procedure are purely related to the synthesis of the control law, whilst the last two are related to the building of the virtual environment. In the spirit of a personalized medicine, we could imagine to *substitute* Step 1) with a real T2DM subject, undergoing a real clinical non-invasive experiment (like the IVGTT, usually exploited for such aim [34]) in order to identify the DDE compact model parameters. Instead, here we consider the case of a general control law, designed upon an average VP that could be the representative of a rather heterogenous class of T2DM subjects: a unique control law applied in closed-loop to different individuals, each belonging to the same class of patients.

TABLE I
DDE MODEL PARAMETERS. REFER TO SECTION 2 FOR THE MEASUREMENT UNITS.

$$G_b = 8.45 \quad I_b = 47.85 \quad T_{iGmax} = 1.695$$
$$\gamma = 15.92 \quad G^* = 9 \quad \tau_g = 6.5$$
$$V_G = 0.18 \quad K_{xi} = 3.8 \cdot 10^{-2} \quad T_{gh} = 0.0023$$
$$V_I = 0.25 \quad K_{xgi} = 3.15 \cdot 10^{-5}$$

A. Design of the output dynamic regulator

Choosing $G_{ref} = 5$ mM, from (4), we obtain $I_{ref} = 81.13$ pM and $v_{ref} = 0.77$ pmol/kgBW/min. By setting the numeric values of H_1, H_2, H_3 and ρ as follow

$$\begin{array}{ll} H_1 = 2.2 \cdot 10^{-3}, & H_2 = -8.66, \\ H_3 = 5.7 \cdot 10^{-2}, & \rho = 2 \cdot 10^{-5}. \end{array} \tag{48}$$

according to the constraints of Assumption 2, one possible choice for the other control parameters, is given by

$$\begin{array}{l} p_1 = p_2 = 2, \quad q_1 = q_2 = q_3 = q_4 = 10^{-7}, \quad \omega_1 = 40, \\ \omega_2 = 1, \quad \omega_3 = 30, \quad \omega_4 = 3, \quad \eta = 10^{-3}, \quad \mu = 10^{-3}. \end{array} \tag{49}$$

Assumption 1 is also satisfied: the initial state of the glucose-insulin system may be supposed as a constant function with the usual hypothesis of plasma glycemia and insulinemia fixed at their basal values before the insulin administration therapy starts; regards to the initial condition of the regulator, it is set by the designer as a constant function fixed at the estimates of basal glycemia and insulinemia. Indeed such an initialization ensures Assumption 1 and provides the following initial conditions for the closed-loop system (2), (6):

$$\begin{bmatrix} G_0(\tau) \\ I_0(\tau) \\ \widehat{G}_0(\tau) \\ \widehat{I}_0(\tau) \end{bmatrix} \equiv \begin{bmatrix} G_b \\ I_b \\ \widehat{G}_b \\ \widehat{I}_b \end{bmatrix} = \begin{bmatrix} 8.45 \\ 47.85 \\ 7.75 \\ 73.80 \end{bmatrix}, \qquad \tau \in [-\tau_g, 0]. \tag{50}$$

with the estimates $\widehat{G}_b$, $\widehat{I}_b$ set with displacements that are larger than 8% and 50% for G_b and I_b, respectively. In summary, all the assumptions, needed to apply the theoretical result stated in Theorem 1, are satisfied for the average VP.

B. Implementation of the closed-loop control law

Before to get in the details of the virtual environment, there are a couple of implementation issues to be properly taken into account. The former regards how to cope with possibly negative control inputs. From the one hand, the control law is designed without imposing any constraint on the positivity of the input signal; on the other hand, the control input is provided by an exogenous insulin delivery rate that clearly cannot become negative. Therefore, anytime the control algorithm suggests to deliver a negative input, the feedback is switched off in the simulator and no input is delivered. A way to anticipate (and avoid) these drawbacks is to properly tune the control parameters, trying to drive the control law according to smooth trajectories. Indeed, these drawbacks are easier to occur according to a coarse sampling period.

Another (more technical) point to be considered is how to cope with delayed measurements. These are clearly required by the output dynamic regulator according to the emulator approach (for instance, $v(t_j)$ requires $\bar{y}(t_j - \tau_g)$ in (6)) but, unfortunately, they are available only if assuming a fixed sampling period δ, and that the delay of the model τ_g is a multiple of δ. Of course there are technological constraints that prevent such hypotheses (e.g. the sampling period cannot be chosen small at ease), therefore the implementable control law is required to substitute the delayed measurement $\bar{y}(t_j - \tau_g)$ with an estimate $\hat{y}(t_j - \tau_g)$. A simple solution is to consider the interpolation between the two closest available measurements, i.e. (see [38])

$$\begin{array}{l} \hat{y}(t_j - \tau_g) = \bar{y}_k + \frac{\bar{y}_{k+1} - \bar{y}_k}{t_{k+1} - t_k}(t_j - \tau_g - t_k), \\ t_k = \max\limits_{l \in N} \{ t_l \in \pi_{a,\delta} \, : \, t_l \leq t_j - \tau_g \}. \end{array} \tag{51}$$

In Fig. 1, a simulation of the closed-loop system (15) with uniform sampling period $\delta = 10$ min is reported (a sampling period in accordance to usual Continuous Glucose Monitoring (CGM) systems, as well as to the one chosen in the previous literature [15], [18], [22], [33], [40]). It can be appreciated that, despite the control law is forced to switch off soon after the first half hour, the proposed simulation shows good performances since plasma glycemia is constrained below 5mM within the first 2 hours of the treatment, according to a smooth trajectory that avoids dangerous glucose oscillations. This behavior is confirmed by any other choice of the initial conditions (simulations not reported).

C. Building of the virtual environment

Similarly to [33], a population of $10,000$ T2DM patients is generated by randomly sampling the comprehensive model parameters according to log-normal distributions. All parameters share the same Coefficient of Variation $CV = 5\%$, thus providing a rather heterogeneous population of T2DM patients.

Three distinct scenarios have been considered for VPs under closed-loop glucose control.

[A] Scenario **[A]** refers to VPs at rest monitored for 6 hours after the onset of the exogenous insulin administration.

[B] Scenario **[B]** refers to VPs that receive a single meal during closed-loop control, and is inspired to [43]. The

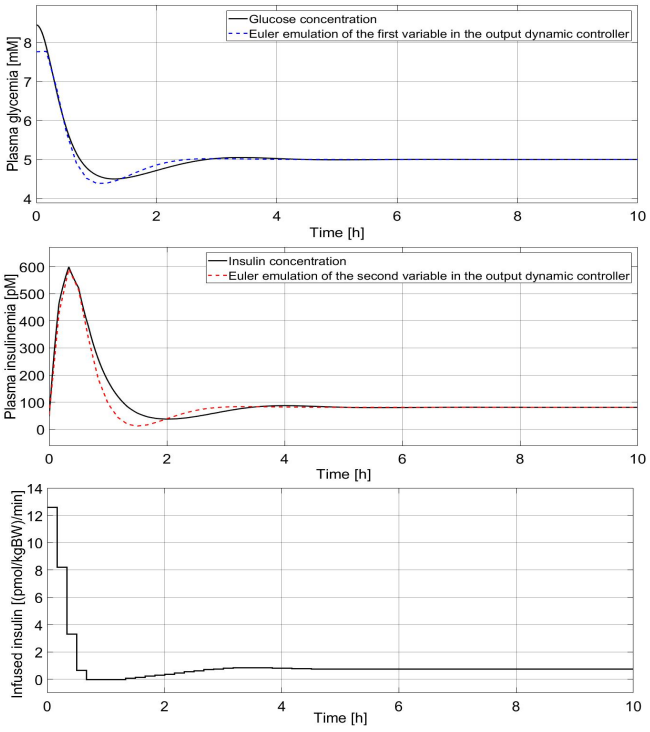

Fig. 1. Simulation of glucose-insulin DDE model in closed-loop with the proposed glucose controller with a sampling period $\delta = 10$ min. In the first two upper panels the continuous lines refer to the glucose and insulin concentrations, whilst the dotted lines refer the linear interpolations of discrete-time available values $\widehat{G}(j\delta)$ (blue dotted line), $\widehat{I}(j\delta)$ (red dotted line), $j = 0, 1, ...$ The third panel reports the input signal.

monitoring lasts for 24 hours: the control law is applied at time 0h, and the VP is supposed to have reached the controlled normoglycemic steady-state after 8 hours. Then a meal is administered and the VP is monitored for the remaining 16 hours. The meal is treated as an unknown disturbance by the closed-loop system, and is modeled by means of the gastro-intestinal tract of [9] providing the glucose appearance rate $d(t)$ straightforwardly in the glucose dynamics. Three different single meals are here considered: 60, 90 and 120 g of CHO.

[C] Scenario **[C]** aims at replicating the daily three meals administration on VPs, and is inspired by [9]. It lasts 24 hours, with the VP supposed to be administered the exogenous insulin therapy at time 0h as in Scenario **[B]** and, then, three meals of 45 g, 70 g and 70 g are administered at 8h, 12h and 20h, respectively.

Remark 2: According to [43], Scenario **[B]** considers a 16 hours monitoring period after meal administration to detect and evaluate on the long period possible hypoglycemia cases due to excesses of insulin administration stimulated by the large CHO content of the meals (and not balanced by further meals).

Three fixed sampling periods have been chosen, according to the available CGM technology and to past literature, [15], [18], [22], [33], [40]: $\delta = 5$ min, $\delta = 10$ min and $\delta = 15$ min.

Errors in blood glucose measurements and malfunctioning of the insulin delivery pumps are also considered, in order to simulate most common uncertainties affecting the artificial pancreas devices. More in details, similarly to [33], if $\bar{y}_j$ and $v(t_j)$ are the ideal measurement acquired at t_j and the input to be administered and held in the time interval $[t_j, t_{j+1})$, what will be actually exploited in the feedback control law are $\tilde{y}_j$ and $\tilde{v}(t_j)$, provided by:

$$\begin{aligned} \tilde{y}_j &= \bar{y}_j + CV_g \bar{y}_j N_j, \\ \tilde{v}(t_j) &= v(t_j) + CV_v v(t_j) M_j, \end{aligned} \tag{52}$$

where N_j and M_j are sequences of independent, zero-mean Gaussian random variables with unitary variance, and $CV_g = 5\%$, $CV_v = 15\%$ are the coefficient of variation (see [3], [33]).

Remark 3: Besides within the output dynamic regulator, noisy measurements in (52) have been exploited also to assess safety and efficacy criteria on VPs simulation.

D. Safety/efficiency criteria

Safety and efficiency criteria are exploited to evaluate the glucose control law when applied to a VP or to a population of VPs. They are both inspired by [3]. Regards to safety, there is substantially a unique mandatory requirement: plasma glycemia must never become smaller than a safety threshold (i.e. the exogenous insulin must not be administered in excess to avoid hypoglycemia cases). We set two thresholds: a VP simulation with plasma glycemia below 3.3mM (even for just one single glucose measurement) will be labelled as a *hypoglicemic* case; if plasma glycemia goes below 2mM, it will be labelled as a *severe hypoglycemic* case. Table II reports how to evaluate the safety criteria on a population of VPs [3]. It is apparent that even a single case of severe hypoglycemia is sufficient to highlight the failure of the insulin administration therapy.

TABLE II
SAFETY CRITERIA

Safety criteria	**Conditions**
excellent safety	no cases of severe hypoglycemia no cases of hypoglycemia
good safety	no cases of severe hypoglycemia less than 5% cases of hypoglycemia
satisfactory safety	no cases of severe hypoglycemia less than 20% cases of hypoglycemia
unsafe	any other case

Efficacy criteria aim at evaluating the ability of the output glucose control law to drive (and keep) plasma glucose concentration within suitable normoglycemia domains. Each VP simulation is assigned a *label* of *excellent/good/satisfactory/unsatisfactory efficacy* according to the criteria summarized in Tables III and IV for VPs at rest or during a meal, respectively. Regards to VPs at rest, efficacy criteria investigate whether plasma glycemia is definitely constrained below a certain level within the first 3 hours of treatment. During a meal, efficacy criteria evaluate the control law capability to definitely lower the (physiological) postprandial hyperglycemic state down to a suitable level within the first 2 hours after the meal ingestion.

A different way to assess efficacy is to assign to the VP a fraction of each labels, provided by the percentage of glucose samples that comply with the efficacy label. For VPs at rest, such a percentage is computed on the interval [3h,6h], for the single meals administration, the percentage is computed on the interval [10h,12h], whilst for the 3 meals administration scenario, the percentage is computed on the intervals [10h,12h]∪[14h,20h]∪[22h,24h]. Thus, for instance, a simulation on a VP at rest provides 0.85 of excellent efficacy if 85% of the glucose samples after the first 3 hours of the insulin administration therapy is constrained below 6mM, and 0.15 of good efficacy if 15% of the glucose samples after the first 3 hours of the insulin administration therapy is constrained within 6mM and 7mM. Both *label* and *fractional* efficacy criteria are accounted for in the proposed simulations.

TABLE III
EFFICACY CRITERIA FOR A VP AT REST

Efficacy criteria	**Conditions after the first 3h of treatment**
excellent	$G < 6$mM
good	$6\text{mM} \leq G < 7\text{mM}$
satisfactory	$7\text{mM} \leq G < 8\text{mM}$
unsatisfactory	$G \geq 8$mM

TABLE IV
EFFICACY CRITERIA FOR A VP DURING MEALS

Efficacy criteria	**Conditions after 2h from meal and during the period before the possible next meal**
excellent	$G < 8$mM
satisfactory	$8\text{mM} \leq G < 11\text{mM}$
unsatisfactory	$G \geq 11$mM

An efficient visual representation for the VPs population undergoing the proposed AP therapy is provided by the *Control-Variability Grid Analysis* (CVGA) (see e.g. [22], [23], [33], [43]). The grid allows to visualize the largest glucose excursions produced by the control algorithm: each point of the grid is a VP and indicates the minimum (reversed X-axis) and maximum (Y-axis) blood glucose values within the considered time period. The grid, on which the data points are plotted, is composed by nine square zones (see Table V) used in order to classify the controller's performances.

TABLE V
CONTROL VARIABILITY GRID ANALYSIS

Grid zone	**Control performances**
A	accurate control
Lower B	benign deviations into hypoglycemia
B	benign control deviations
Upper B	benign deviations into hyperglycemia
Lower C	over-correction of hyperglycemia
Upper C	over-correction of hypoglycemia
Lower D	failure to deal with hypoglycemia
Upper D	failure to deal with hyperglycemia
E	erroneous control

E. Data analysis and discussion

As a preliminary test we apply the closed-loop control on the average VP (the one exploited to estimate the DDE compact model parameters, upon which the model-based control is designed). Figs. 2 and 3 report simulations that refer to Scenarios **[A]** and **[B]** (120 g of CHO), respectively, with a sampling period $\delta = 10$ min. In both scenarios we never have hypoglycemia cases and very good efficacy results: fractional efficacy results for Scenario **[B]** are reported in Table VI.

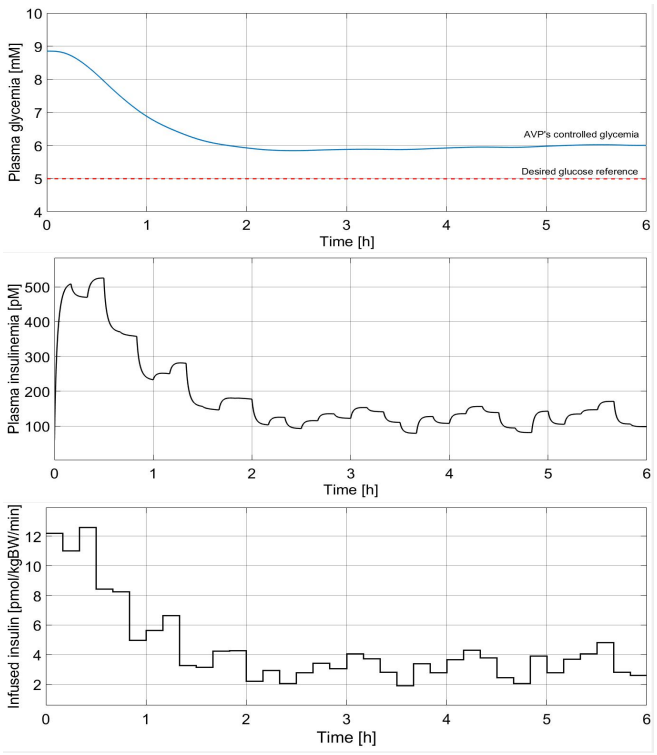

Fig. 2. Plasma glycemia (upper panel), plasma insulinemia (middle panel) and insulin infusion rate (lower panel) for the average VP during 6 hours of treatment (no meal administration, Scenario **[A]**). A sampling period of 10 min is considered.

TABLE VI
FRACTIONAL EFFICACY RESULTS FOR THE AVERAGE VP WITH A SINGLE MEAL (SCENARIO B)

Meal	**Sampling period**	**Excellent**	**Satisfactory**	**Unsatisfactory**
60 g	$\delta = 5$ min	68%	32%	0%
90 g	$\delta = 5$ min	56%	44%	0%
120 g	$\delta = 5$ min	48%	52%	0%
60 g	$\delta = 10$ min	69%	31%	0%
90 g	$\delta = 10$ min	62%	38%	0%
120 g	$\delta = 10$ min	61.5%	30.8%	7.7%
60 g	$\delta = 15$ min	56%	44%	0%
90 g	$\delta = 15$ min	56%	44%	0%
120 g	$\delta = 15$ min	56%	33%	11%

Regards to the 10,000 VPs population, all three scenarios share an excellent safety results: no hypoglycemic cases occur, regardless of the sampling period $\delta \in \{5, 10, 15\}$ min, regardless whether the VP is at rest or a meal is administered and, in this last case case, regardless of the amount of the meal. Pictures of glycemia envelopes are reported in Figs. 4, 5 and 6 for scenarios **[A]**, **[B]** and **[C]**, respectively, with $\delta = 10$ min. Efficacy results are resumed in Tables VII, VIII and IX

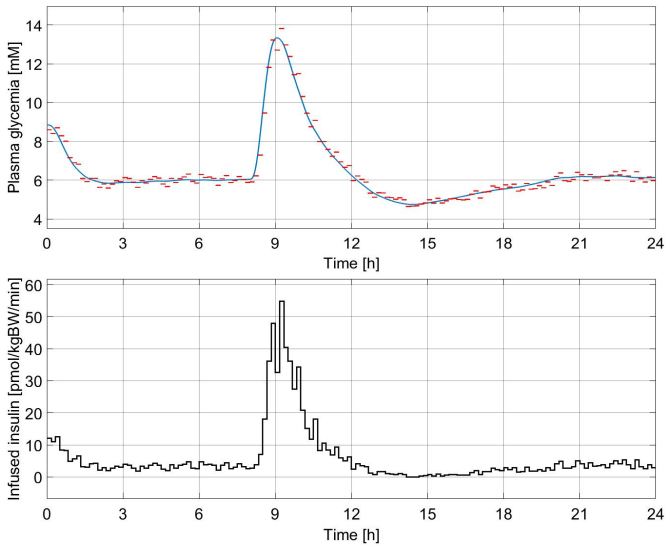

Fig. 3. Plasma glycemia and insulin infusion rate for the average VP during the whole 24 h of the virtual experiment (meal of 120 [g] CHO, Scenario **[B]**). Red lines are the noisy glucose samples measurements in each sampling interval and blue continuous line is the VP controlled glycemia. The piecewise-constant black line is the control input with $\delta = 10$min.

for scenarios **[A]**, **[B]** and **[C]**, respectively. Finally, the 10,000 VPs simulations are recap in the CGVAs, see Fig. 7 and Tables X, XI, XII for Scenario **[B]**, and Fig. 8 and Table XIII for Scenarios **[C]**.

As far as the efficacy results, the common denominator of the three scenarios is that there are no unsatisfactory results, with a dominant percentage of excellent vs good/satisfactory when dealing with fractional efficacy. Efficacy seems to strengthen when the sampling period becomes coarser. This fact, though counterintuitive (because a coarser sampling period is associate to coarser Euler emulation of the control law), is coherent with the feedback control scheme: a larger sampling period means a larger period of the sample-and-hold regulator, therefore a possible initial high insulin administration may be held for a longer time. These efficacy benefits have to cope with the side-effects possibly affecting the safety, since a larger administration of insulin is not balanced by any exogenous counter-regulating hormone (like glucagon). However, these facts do not affect the excellent safety results since no VP ever undergoes hypoglycemic cases in all reported simulations. The CVGAs confirm the goodness of the closed-loop control, highlighting that only during the largest meal administration (of 120 g of CHO) a low percentage of VP is found in the lower D zone (spanning from 0.39% for $\delta = 5$ to 2.16% for $\delta = 15$ min), though according to a minimum plasma glycemia always grater than 60 mM.

Remark 4: As a final remark, in all simulations, the control input never exceeds 80 pmol/kgBW/min, corresponding to $5,600$ pmol/min for a VP of an average weight of 70kg. Although literature on artificial pancreas reports a limit of 4U/h for the insulin infusion rate [3], corresponding to about 466 pmol/min, our control input amplitude is still acceptable, according to the high-dose insulin protocols employed in the treatment of severe beta-blocker and calcium channel-blocker

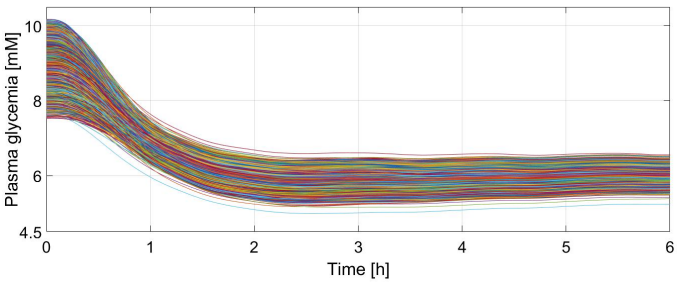

Fig. 4. Controlled glycemia of a 10,000 VPs population at rest (Scenario **[A]**), sampling period $\delta = 10$ min.

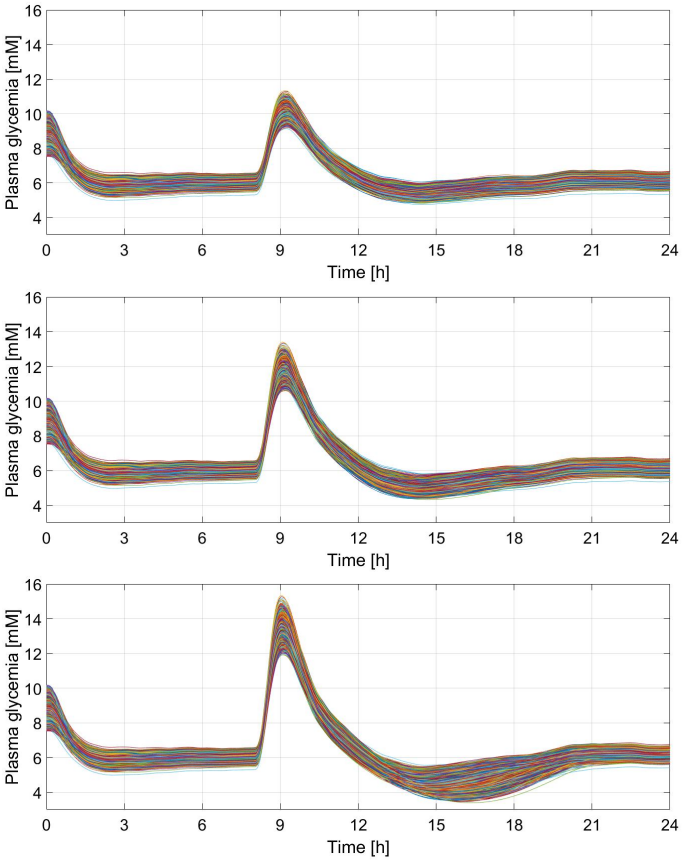

Fig. 5. Controlled glycemia of a 10,000 VPs population according to Scenario **[B]**: 60 g (upper panel), 90 g (medium panel) and 120 g (lower panel). Sampling period $\delta = 10$ min.

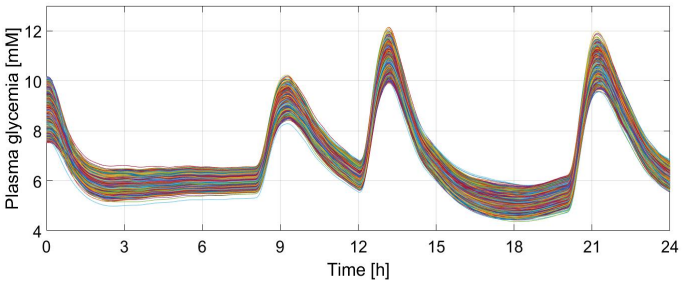

Fig. 6. Controlled glycemia of a 10,000 VPs population according to Scenario **[C]**. Sampling period $\delta = 10$ min.

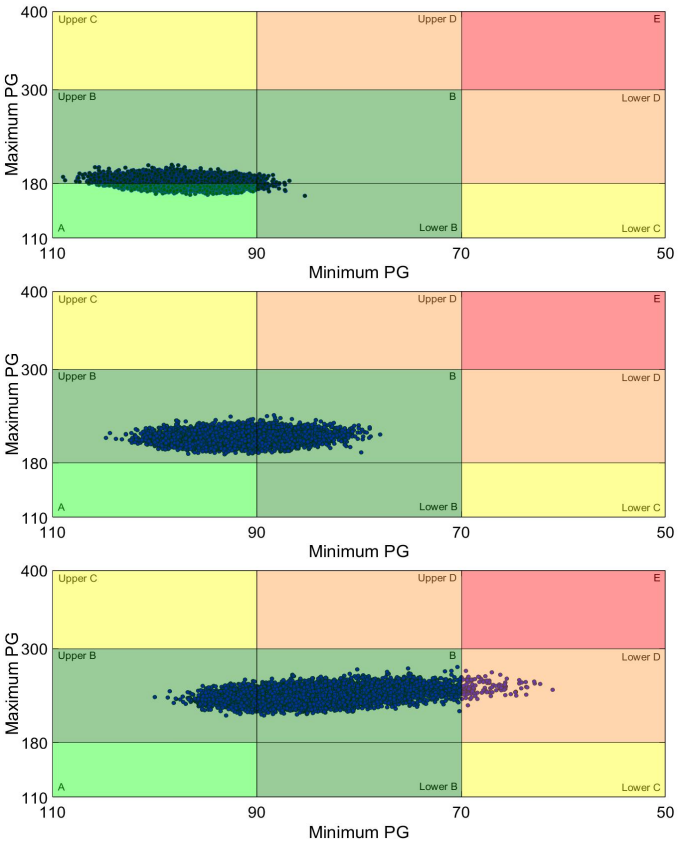

Fig. 7. Control-variability grid of the control law action on a population of $10,000$ VPs, Scenario **[B]**: 60 g (upper panel), 90 g (middle panel) and 120 g (lower panel) of CHO administered. Sampling period $\delta = 10$ min.

poisoning with insulin infusion ranges up to 22U/kgBW/h (about $180,000$ pmol/min), [16], a much larger upper bound than the one reported by simulations.

VI. Conclusion

In this paper, the recent results about stabilization in the sample-and-hold sense, for time-delay systems, have been used in order to cope with the problem related to the tracking of a desired plasma glucose concentration by means of intra-

TABLE VII
LABEL AND FRACTIONAL EFFICACY RESULTS FOR THE 10,000 VPS POPULATION AT REST (SCENARIO **[A]**)

Efficacy	**Label**	**Fractional**	**Sampling period**
excellent	3.95%	61.61%	$\delta = 5$ min
good	96.05%	38.39%	$\delta = 5$ min
satisfactory	0%	0%	$\delta = 5$ min
unsatisfactory	0%	0%	$\delta = 5$ min
excellent	4.30%	55.40%	$\delta = 10$ min
good	95.70%	44.60%	$\delta = 10$ min
satisfactory	0%	0%	$\delta = 10$ min
unsatisfactory	0%	0%	$\delta = 10$ min
excellent	9.00%	60.85%	$\delta = 15$ min
good	91.00%	39.15%	$\delta = 15$ min
satisfactory	0%	0%	$\delta = 15$ min
unsatisfactory	0%	0%	$\delta = 15$ min

TABLE VIII
LABEL AND FRACTIONAL EFFICACY RESULTS FOR THE 10,000 VPS POPULATION (SCENARIO **[B]**)

Efficacy	**Label**	**Fractional**	**Meal**	**Sampling period**
excellent	0%	99.86%	60g	$\delta = 5$ min
satisfactory	100%	0.14%	60g	$\delta = 5$ min
unsatisfactory	0%	0%	60g	$\delta = 5$ min
excellent	0%	99.99%	60g	$\delta = 10$ min
satisfactory	100%	0.01%	60g	$\delta = 10$ min
unsatisfactory	0%	0%	60g	$\delta = 10$ min
excellent	0%	100%	60g	$\delta = 15$ min
satisfactory	100%	0%	60g	$\delta = 15$ min
unsatisfactory	0%	0%	60g	$\delta = 15$ min
excellent	0%	85.68%	90g	$\delta = 5$ min
satisfactory	100%	14.32%	90g	$\delta = 5$ min
unsatisfactory	0%	0%	90g	$\delta = 5$ min
excellent	0%	97.16%	90g	$\delta = 10$ min
satisfactory	100%	2.84%	90g	$\delta = 10$ min
unsatisfactory	0%	0%	90g	$\delta = 10$ min
excellent	0%	99.06%	90g	$\delta = 15$ min
satisfactory	100%	0.94%	90g	$\delta = 15$ min
unsatisfactory	0%	0%	90g	$\delta = 15$ min
excellent	0%	52.43%	120g	$\delta = 5$ min
satisfactory	100%	47.57%	120g	$\delta = 5$ min
unsatisfactory	0%	0%	120g	$\delta = 5$ min
excellent	0%	94.96%	120g	$\delta = 10$ min
satisfactory	100%	5.04%	120g	$\delta = 10$ min
unsatisfactory	0%	0%	120g	$\delta = 10$ min
excellent	0%	99.43%	120g	$\delta = 15$ min
satisfactory	100%	0.57%	120g	$\delta = 15$ min
unsatisfactory	0%	0%	120g	$\delta = 15$ min

TABLE IX
LABEL AND FRACTIONAL EFFICACY RESULTS FOR THE 10,000 VPS POPULATION (SCENARIO **[C]**)

Efficacy	**Label**	**Fractional**	**Sampling period**
excellent	0%	100%	$\delta = 5$ min
satisfactory	100%	0%	$\delta = 5$ min
unsatisfactory	0%	0%	$\delta = 5$ min
excellent	0%	100%	$\delta = 10$ min
satisfactory	100%	0%	$\delta = 10$ min
unsatisfactory	0%	0%	$\delta = 10$ min
excellent	0%	100%	$\delta = 15$ min
satisfactory	100%	0%	$\delta = 15$ min
unsatisfactory	0%	0%	$\delta = 15$ min

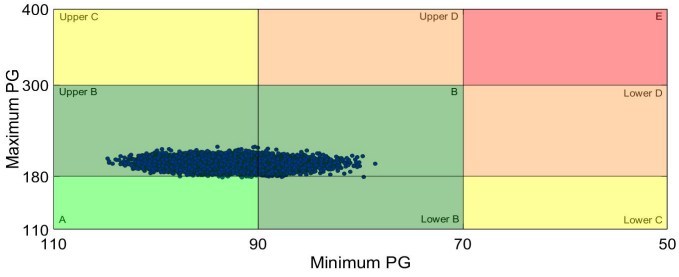

Fig. 8. Control-variability grid of the control law action on a population of $10,000$ VPs, Scenario **[C]**. Sampling period $\delta = 10$ min.

TABLE X
CVGA RESULTS FOR THE 10,000 VPS POPULATION (SCENARIO **[B]**, MEAL OF $60g$ CHO)

Grid zone	Controller results	Sampling period
A	46.78%	$\delta = 5$ min
Lower B	0.09%	$\delta = 5$ min
B	0.02%	$\delta = 5$ min
Upper B	53.11	$\delta = 5$ min
Lower C	0%	$\delta = 5$ min
Upper C	0%	$\delta = 5$ min
Lower D	0%	$\delta = 5$ min
Upper D	0%	$\delta = 5$ min
E	0%	$\delta = 5$ min
A	34.72%	$\delta = 10$ min
Lower B	0.31%	$\delta = 10$ min
B	0.4%	$\delta = 10$ min
Upper B	64.57%	$\delta = 10$ min
Lower C	0%	$\delta = 10$ min
Upper C	0%	$\delta = 10$ min
Lower D	0%	$\delta = 10$ min
Upper D	0%	$\delta = 10$ min
E	0%	$\delta = 10$ min
A	18.6%	$\delta = 15$ min
Lower B	0.13%	$\delta = 15$ min
B	0.3%	$\delta = 15$ min
Upper B	80.97%	$\delta = 15$ min
Lower C	0%	$\delta = 15$ min
Upper C	0%	$\delta = 15$ min
Lower D	0%	$\delta = 15$ min
Upper D	0%	$\delta = 15$ min
E	0%	$\delta = 15$ min

TABLE XI
CVGA RESULTS FOR THE 10,000 VPS POPULATION (SCENARIO **[B]**, MEAL OF $90g$ CHO)

Grid zone	Controller results	Sampling period
A	0%	$\delta = 5$ min
Lower B	0%	$\delta = 5$ min
B	11.99%	$\delta = 5$ min
Upper B	88.01%	$\delta = 5$ min
Lower C	0%	$\delta = 5$ min
Upper C	0%	$\delta = 5$ min
Lower D	0%	$\delta = 5$ min
Upper D	0%	$\delta = 5$ min
E	0%	$\delta = 5$ min
A	0%	$\delta = 10$ min
Lower B	0%	$\delta = 10$ min
B	27.02%	$\delta = 10$ min
Upper B	72.98%	$\delta = 10$ min
Lower C	0%	$\delta = 10$ min
Upper C	0%	$\delta = 10$ min
Lower D	0%	$\delta = 10$ min
Upper D	0%	$\delta = 10$ min
E	0%	$\delta = 10$ min
A	0%	$\delta = 15$ min
Lower B	0%	$\delta = 15$ min
B	25.05%	$\delta = 15$ min
Upper B	74.95%	$\delta = 15$ min
Lower C	0%	$\delta = 15$ min
Upper C	0%	$\delta = 15$ min
Lower D	0%	$\delta = 15$ min
Upper D	0%	$\delta = 15$ min
E	0%	$\delta = 15$ min

TABLE XII
CVGA RESULTS FOR THE 10,000 VPS POPULATION (SCENARIO **[B]**, MEAL OF $120g$ CHO)

Grid zone	Controller results	Sampling period
A	0%	$\delta = 5$ min
Lower B	0%	$\delta = 5$ min
B	65.99%	$\delta = 5$ min
Upper B	33.62	$\delta = 5$ min
Lower C	0%	$\delta = 5$ min
Upper C	0%	$\delta = 5$ min
Lower D	0.39%	$\delta = 5$ min
Upper D	0%	$\delta = 5$ min
E	0%	$\delta = 5$ min
A	0%	$\delta = 10$ min
Lower B	0%	$\delta = 10$ min
B	84.01%	$\delta = 10$ min
Upper B	14.81%	$\delta = 10$ min
Lower C	0%	$\delta = 10$ min
Upper C	0%	$\delta = 10$ min
Lower D	1.18%	$\delta = 10$ min
Upper D	0%	$\delta = 10$ min
E	0%	$\delta = 10$ min
A	0%	$\delta = 15$ min
Lower B	0%	$\delta = 15$ min
B	83.66%	$\delta = 15$ min
Upper B	14.18%	$\delta = 15$ min
Lower C	0%	$\delta = 15$ min
Upper C	0%	$\delta = 15$ min
Lower D	2.16%	$\delta = 15$ min
Upper D	0%	$\delta = 15$ min
E	0%	$\delta = 15$ min

TABLE XIII
CVGA RESULTS FOR THE 10,000 VPS POPULATION (SCENARIO **[C]**)

Grid zone	Controller results	Sampling period
A	0.27%	$\delta = 5$ min
Lower B	0.29%	$\delta = 5$ min
B	24.64%	$\delta = 5$ min
Upper B	74.8	$\delta = 5$ min
Lower C	0%	$\delta = 5$ min
Upper C	0%	$\delta = 5$ min
Lower D	0%	$\delta = 5$ min
Upper D	0%	$\delta = 5$ min
E	0%	$\delta = 5$ min
A	0.08%	$\delta = 10$ min
Lower B	0.03%	$\delta = 10$ min
B	19.89%	$\delta = 10$ min
Upper B	80%	$\delta = 10$ min
Lower C	0%	$\delta = 10$ min
Upper C	0%	$\delta = 10$ min
Lower D	0%	$\delta = 10$ min
Upper D	0%	$\delta = 10$ min
E	0%	$\delta = 10$ min
A	0%	$\delta = 15$ min
Lower B	0%	$\delta = 15$ min
B	22.85%	$\delta = 15$ min
Upper B	77.15%	$\delta = 15$ min
Lower C	0%	$\delta = 15$ min
Upper C	0%	$\delta = 15$ min
Lower D	0%	$\delta = 15$ min
Upper D	0%	$\delta = 15$ min
E	0%	$\delta = 15$ min

venous insulin administration for T2DM patients. A semi-global sampled-data output controller for the glucose-insulin system is proposed. It is shown that emulation, by Euler approximation, of the provided semi-global nonlinear output dynamic controller yields the reduction of a high basal plasma glucose concentration to a reference glucose value. The control law has been evaluated by closing the loop on a population of 10,000 virtual patients, generated by a model recently accepted by the Food and Drug Administration (FDA) as an alternative to animal trials for the preclinical testing of control strategies in artificial pancreas. Criteria to evaluate the performances of the proposed control law have been taken into account in the data analysis. The simulations and the criteria adopted for the data analysis show the good performances of the proposed control strategy.

REFERENCES

[1] A. Borri, F. Cacace, A. De Gaetano, A. Germani, C. Manes, P. Palumbo, S. Panunzi, Luenberger-Like Observers for Nonlinear Time-Delay Systems with Application to the Artificial Pancreas, *IEEE Control Systems Magazine*, vol. 37(4), 2017, pp 33-49.

[2] D. Carnevale, A. R. Teel and D. Nesic, "A Lyapunov proof of an improved maximum allowable transfer interval for networked control systems", *IEEE Trans. Automat. Control*, vol. 52, 2007, pp 892-897.

[3] L. J. Chassin, M. E. Wilinska, R. Hovorka, "Evaluation of glucose controllers in virtual environment: methodology and sample application", *Artif. Intell. Med.*, vol. 32, 2004, pp 171-181.

[4] F. Chee, A. V. Savkin, T.L. Fernando, S. Nahavandi, Optimal H-infinity insulin injection control for blood glucose regulation in diabetic patients, *IEEE Trans. on Biomedical Engineering*, vol. 52, 2005, pp 1625-1631.

[5] F. H. Clarke, "Discontinuous feedback and nonlinear systems", *Plenary Lecture at IFAC Conference on Nonlinear Control Systems*, 2010.

[6] F. H. Clarke, Y. S. Ledyaev, E. D. Sontag, A. I. Subbotin, "Asymptotic controllability implies feedback stabilization", *IEEE Trans. Automat. Control*, vol. 42, 1997, pp 1394-1407.

[7] C. Cobelli, E. Renard, B. Kovatchev, Artificial pancreas: past, present, future, *Diabetes*, vol. 60, 2011, pp 2672-2682.

[8] C. Dalla Man, D.M. Raimondo, R.A. Rizza, C. Cobelli, "GIM, simulation software of meal glucose-insulin model", *J. Diabetes Sci. Technol.*, vol. 1(3), 2007, pp 323-330.

[9] C. Dalla Man, R.A. Rizza, C. Cobelli, "Meal simulation model of the glucose-insulin system", *IEEE Trans. Biomed. Eng.*, vol. 54, 2007, pp 1740-1749.

[10] M. Di Ferdinando, P. Pepe, "Robustification of Sample-and-Hold Stabilizers for Control-Affine Time-Delay Systems", *Automatica*, vol. 83, 2017, pp 141-154.

[11] M. Di Ferdinando, P. Pepe, "On Emulation of Observer-Based Stabilizers for Nonlinear Systems", *56th IEEE Conference on Decision and Control*, Melbourne, Australia, 2017, pp 6738-6743.

[12] M. Di Ferdinando, P. Pepe, "On Euler Emulation of Observer-Based Stabilizers for Nonlinear Time-Delay Systems", *Arxiv*.

[13] M. Di Ferdinando, P. Pepe, P. Palumbo, S. Panunzi, A. De Gaetano, "Robust Global Nonlinear Sampled-Data Regulator for the Glucose-Insulin System", *56th IEEE Conference on Decision and Control*, Melbourne, Australia, 2017, pp 4686-4691.

[14] F. J. Doyle III, L.M. Huyett, J.B. Lee, H.C. Zisser, E. Dassau, "Closed-Loop Artificial Pancreas Systems: Engineering the Algorithms", *Diabetes Care*, vol. 37, 2014, pp 1191-1197.

[15] P. Dua, F.J. Doyle III, E.N. Pistikopoulos, "Model-based blood glucose control for Type 1 diabetes via parametric programming", *IEEE Trans. Biomed. Eng.*, vol. 53, 2006, pp 1478-1491.

[16] K. M. Engebretsen, K. M. Kaczmarek, J. Morgan, J. S. Holger, "High-dose insulin therapy in beta-blocker and calcium channel-blocker poisoning", *Clin. Toxicol.*, vol. 49, 2011, pp 277-283.

[17] E. Fridman, "Introduction to Time-Delay Systems: Analysis and Control", *Birkhauser*, 2014.

[18] R. Hovorka, "Closed-loop insulin delivery: From bench to clinical practice", *Nature Rev. Endocrinol.*, vol. 7(7), 2011, pp 385-395.

[19] L. Kovàcs, P. Szalay, Z. Almàssy, L. Barkai, "Applicability Results of a Nonlinear Model-Based Robust Blood Glucose Control Algorithm", *J. Diabetes Science and Technology*, vol. 7(3), 2013, pp 708-716.

[20] B. P. Kovatchev, M. D. Breton, C. Dalla Man, C. Cobelli, "In Silico Model and Computer Simulation Environment Approximating the Human Glucose/Insulin Utilization", *Food and Drug Administration Master File MAF 1521*, 2008.

[21] B. P. Kovatchev, W.V. Tamborlane, W.T. Cefalu, C. Cobelli, "The Artificial Pancreas in 2016: A Digital Treatment Ecosystem for Diabetes", *Diabetes Care*, vol. 39, 2016, pp 1123-1126.

[22] L. Magni, D. M. Raimondo, C. Dalla Man, M. Breton, S. Patek, G. De Nicolao, C. Cobelli, B. Kovatchev "Evaluating the efficacy of the closed-loop glucose regulation via control-variability grid analysis", *J Diabetes Sci Technol.* , vol. 2, 2008, pp 630-635.

[23] L. Magni, D. M. Raimondo, C. Dalla Man, G. De Nicolao, B. Kovatchev, C. Cobelli, "Model predictive control of glucose concentration in type I diabetic patients: an in silico trial", *Biomed. Signal Process. Control*, vol. 4, 2009, pp 338-346.

[24] A. Makroglou, J. Li, Y. Kuang, Mathematical models and software tools for the glucose-insulin regulatory system and diabetes: an overview, *Applied Numerical Mathematics*, vol. 56, 2006, pp 559-573.

[25] M. Messori, G.P. Cremona, C. Cobelli, L. Magni, Individualized Model Predictive Control for the Artificial Pancreas, *IEEE Control Systems Magazine*, vol. 38(1), 2018, pp 86-104.

[26] D. Nesic and A. R. Teel, "Sampled-data control of nonlinear systems: an overview of recent results", *Perspectives on Robust Control*, 2001, pp 221-239.

[27] D. Nesic and A. R. Teel, "A framework for stabilization of nonlinear sampled-data systems based on their approximate discrete-time models", *IEEE Trans. Automat. Control*, vol. 49, 2004, pp 1103-1122.

[28] D. Nesic, A. R. Teel and D. Carnevale, "Explicit Computation of the Sampling Period in Emulation of Controllers for Nonlinear Sampled-Data Systems", *IEEE Trans. Automat. Contr.*, vol. 54, 2009, pp 619-624.

[29] K. Ogurtsova, J.D. da Rocha fernandes, Y. Huang, U. Linnenkamp, L. Guariguata, N.H. Cho, D. Cavan, J.E. Shaw, L.E. Makaroff, "IDF Diabetes Atlas: Global estimates for the prevalence of diabetes for 2015 and 2040", *Diabetes Res. Clin. Pract.*, vol. 128, 2017, pp 40-50.

[30] P. Palumbo, S. Ditlevsen, A. Bertuzzi, A. De Gaetano, Mathematical modeling of the glucoseinsulin system: A review, *Math. Biosci.*, vol. 244, 2013, pp 69-81.

[31] P. Palumbo, S. Panunzi, A. De Gaetano, "Qualitative behavior of a family of delay differential models of the glucose insulin system", *Discrete and Continuous Dynam. Systems - B*, vol. 7, 2007, pp 399-424.

[32] P. Palumbo, P. Pepe, S. Panunzi, A. De Gaetano, Time-Delay Model-Based Control of the Glucose-Insulin System, by Means of a State Observer, *European Journal of Control*, vol. 6, 2012, pp 591-606.

[33] P. Palumbo, G. Pizzichelli, S. Panunzi, P. Pepe, A. De Gaetano, Model-based control of plasma glycemia: Tests on populations of virtual patients, *Math. Biosciences*, vol. 257, 2014, pp 2-10.

[34] S. Panunzi, P. Palumbo, A. De Gaetano, "A discrete single delay model for the intra-venous glucose tolerance test", *Theoretical Biology and Medical Modelling*, vol. 4, 2007.

[35] P. Pepe, "On Lyapunov-Krasovskii functionals under Caratheodory conditions", *Automatica J. IFAC*, vol. 43, 2007, pp. 701-706.

[36] P. Pepe, "Stabilization in the sample-and-hold sense of nonlinear retarded systems", *SIAM J. Control Optim.*, vol. 52, 2014, pp 3053-3077.

[37] P. Pepe, "Robustification of nonlinear stabilizers in the sample-and-hold sense", *Journal of The Franklin Institute*, vol. 42, 2015, pp. 1394-1407.

[38] P. Pepe, "On stability preservation under sampling and approximation of feedbacks for retarded systems", *SIAM J. Control Optim.*, vol. 54, 2016, pp 1895-1918.

[39] P. Pepe, P. Palumbo, S. Panunzi, A. De Gaetano, "Local Sampled-Data Control of the Glucose-Insulin System", *IEEE American Control Conference*, Seattle, WA, USA, 2017, pp. 110-115.

[40] G. Reach, G.S. Wilson, , "Can continuous glucose monitoring be used for the treatment of diabetes", *Anal. Chem.*, vol. 64, 1992, pp. A381-A386.

[41] E. RuizVelazquez, R. Femat, D. U. CamposDelgado, Blood glucose control for type I diabetes mellitus: A robust H-infinity tracking problem, *Control Engineering Practice*,vol. 12, 2004, pp. 1179-1195.

[42] G. Van den Berghe, Insulin therapy for the critically ill patient, *Clinical Cornerstone*, vol. 5(2), 2003, pp 56-63.

[43] K. van Heusden, E. Dassau, H. C. Zisser, D. E. Seborg, F.J. Doyle III, "Control-Relevant Models for Glucose Control Using *A Priori* Patient Characteristics", *IEEE Transaction on Biomedical Engineering*, vol. 59, 2012, pp 1839-1849.

[44] K. Zarkogianni, E. Litsa, K. Mitsis, P.-Y. Wu, C.D. Kaddi, C.-W. Cheng, M.D. Wang, K.S. Nikita, A Review of Emerging Technologies for the Management of Diabetes Mellitus, *IEEE Trans. Biomed. Eng.*, vol. 62(12), 2015, pp 2735-2749.